Summer 2023

Structural and Thermodynamic Studies of Antibody Binding to Blood Coagulation Factor VIII

Jordan Vaughan
Western Washington University, vaughaj5@wwu.edu

Structural and Thermodynamic Studies of Antibody Binding to Blood Coagulation Factor VIII

By

Jordan D. Vaughan

Accepted in Partial Completion

of the Requirements for the Degree

Master of Science

ADVISORY COMMITTEE

Chair, Dr. P. Clint Spiegel

Dr. John Antos

Dr. Spencer Anthony-Cahill

GRADUATE SCHOOL

David L. Patrick, Dean

Master's Thesis

In presenting this thesis in partial fulfillment of the requirements for a master's degree at Western Washington University, I grant to Western Washington University the non-exclusive royalty-free right to archive, reproduce, distribute, and display the thesis in any and all forms, including electronic format, via any digital library mechanisms maintained by WWU.

I represent and warrant this is my original work and does not infringe or violate any rights of others. I warrant that I have obtained written permissions from the owner of any third party copyrighted material included in these files.

I acknowledge that I retain ownership rights to the copyright of this work, including but not limited to the right to use all or part of this work in future works, such as articles or books.

Library users are granted permission for individual, research and non-commercial reproduction of this work for educational purposes only. Any further digital posting of this document requires specific permission from the author.

Any copying or publication of this thesis for commercial purposes, or for financial gain, is not allowed without my written permission.

Signature: *Jordan D. Vaughan*

Date: 7/17/2023

Structural and Thermodynamic Studies of Antibody Binding to Blood Coagulation Factor VIII

A Thesis Presented to

the Faculty of

Western Washington University

In Partial Fulfillment

of the Requirements for the Degree

Master of Science

By

Jordan D. Vaughan

August 2023

Abstract

Blood coagulation factor VIII (FVIII) is a 2332 residue glycoprotein expressed in endothelial cells and plays a significant role in the formation of blood clots. Structurally, FVIII's domains are organized as A1-A2-B-A3-C1-C2. The absence or deficiency of FVIII in the bloodstream gives rise to Hemophilia A; an X-linked bleeding disorder affecting 1 in 5000 males worldwide. To combat this deficiency, patients undergo FVIII replacement therapy which involves frequent injections of FVIII into the bloodstream in the form of blood, plasma, or protein concentrates. Although effective, this treatment commonly results in the development of anti-FVIII inhibitory antibodies in approximately 20-30% of patients.

Across the domains of FVIII, antibody development is most frequently seen for the A2, C2, and A3-C1 domains. Previous crystal structures from the Spiegel lab have led to a wealth of understanding of how inhibitory antibodies interact with the C2 and C1 domains. Two of the crystal structures, those of anti-C2 inhibitors 3E6 and G99, revealed a potential positive cooperation between the two inhibitors stemming from a rigidification of the C2 domain upon G99's binding. Using isothermal titration calorimetry to investigate this, it was determined that these two inhibitors bind the C2 domain independently without any sort of cooperation. Rigidification of the C2 domain upon G99's binding however was proven using this method. Additionally, competition for FVIII binding was investigated for six anti-A2 domain inhibitors. Using bio-layer interferometry, overlap and lack of overlap was identified for five of the six antibodies, illustrating the diversity of the immune response to injected FVIII.

Recent Spiegel lab Cryo-EM structures of have deepened our understanding of how inhibitors bind the C1 and A2 domains to inhibit FVIII. One of such structures is that of human/porcine chimeric construct Et3i bound to the patient-derived antibody NB2E9. In tandem with the data collection for this structure, crystallographic trials were carried out for the isolated C1 domain in complex with the NB2E9 Fab fragment. Despite successful formation of crystals, all failed to diffract.

Acknowledgements

As the SARS-CoV-2 pandemic truly started to prove just how pronounced an effect it would have on our world, I found myself just over a year away from graduating from WWU with a BS in chemistry, a field in which I felt completely lost and directionless in. In May of 2020, I began working at Northwest Laboratory in Bellingham to assist in the handling of nationwide COVID testing. For the first time, I felt as if I was doing something worthwhile in the world of science. It was here that I met incoming Smirnov lab graduate student Melissa Oueld Es Cheikh, who convinced me that I had a chance of admission into the WWU Biochemistry Masters program despite my low GPA should I become involved in undergraduate biochemistry research. After befriending so many current and past Spiegel lab students at NWL and learning about the research of Dr. Spiegel, I was allowed to join the lab in January of 2021. One of such Spiegel alumni I came into contact with was Chris Swanson. Over the course of 2020-2021, he was absolutely instrumental in helping me believe that I could find a place for myself in the world of biochemistry and science as a whole. I cannot thank him enough for his encouragement and near-daily pep talks as I poured my whole being into undoing 4 years of subpar academic performance and engagement to become a worthy candidate for the WWU graduate school.

I must extend my utmost gratitude to Dr. Clint Spiegel for giving me a chance as a graduate student despite my complete lack of biochemistry knowledge. I can hardly believe how much I have evolved as a person and researcher under his tutelage. His granting of total freedom to me to explore the complex world of FVIII biology independently proved essential in my development of critical thinking skills and biochemistry knowledge in general. Dr. Kenny Childers as well helped welcome me into the lab back in January 2021 and was always willing to answer any questions I had, no matter how embarrassingly basic they could sometime be. Fellow graduate student Nathan Avery was the first person in the lab who I truly considered a friend. Over the course of my graduate studies, there was arguably no one more essential to my growth than Nathan. His beyond tireless devotion to our research is unlike anything I have ever seen and I am proud to have worked and learned alongside him as a fellow blood project graduate student. I have no doubts that he will go on to have an incredible career in the world of science, and will prove to be an absolute monster of a graduate student in whatever doctorate program he chooses to pursue.

Juliet McGill was the first undergraduate researcher assigned to me as a graduate student, and continued to work their hardest to assist me and the lab as a whole until the very end. They were a huge help particularly in the department of crystallography, where they continuously made trays never getting discouraged about our lack of diffraction-grade crystals. Corbin Mitchell as well helped me greatly during my first year both with mammalian cell culture training and encouraging a very fun lab atmosphere that really helped make me feel at home in the lab. I wish him the absolute best as he works through his doctoral studies at UCSC. I must also thank Shaun Peters, the former patron saint of the Spiegel lab, for being an incredible source of knowledge as I struggled to learn biochemistry from the ground up. An additional thank you goes out to Ashlee Hoffman, Jess Blair, Justin McGlone, and all of the other current and former Spiegel lab students who supported me during this period.

The whole of the fourth floor has my utmost gratitude as well for making WWU such a wonderful place to be. My sincerest thanks go out to my friends Hanna Kodama, Erich Walkenhauer, and so many other incredible fourth floor residents.

Lastly, I could not have asked for a better, more compassionate partner throughout graduate school than Madeline George. Her boundless support of me and voice of reason were of immense help as I struggled in nearly every way in life over the last few years. I love you.

Table of Contents

List of Tables

List of Figures

List of Abbreviations

A_{280}	Absorbance at 280 nM
ADP	Adenosine diphosphate
ALS	Advanced Light Source
AOF	Animal origin-free
aPCC	Activated Prothrombin Complex Concentrate
aPTT	Activated Plasma Thromboplastin Time
ATP	Adenosine triphosphate
AT	Antithrombin
BCSB	Berkeley Center for Structural Biology
BDD	B-domain-deleted
BLI	Bio-layer Interferometry
BSA	Bovine Serum Albumin
BU	Bethesda Unit
C1	First carboxy-terminal domain of fVIII
C2	Second carboxy-terminal domain of fVIII
CDR	Complimentary Determining Region
CL	Constant light chain region
Cryo-EM	Cryogenic Electron Microscopy

CV	Column Volume
EDTA	Ethylenediaminetetraacetic acid
ELISA	Enzyme-linked Immunosorbent Assay
f8	Gene encoding coagulation factor VIII
Fab	Fragment of antigen binding
Fc	Fragment crystallizable region
FEIBA	Factor Eight Inhibitor Bypassing Activity
F(Roman numeral)	Coagulation factor (Roman numeral) i.e. FVIII (Factor 8)
F(Roman numeral)a	Activated coagulation factor (Roman numeral) i.e. FVIIIa (Activated Factor 8)
FPLC	Fast Protein Liquid Chromatography
FT	Flow-through
GP	Glycoprotein
HBS	HEPES-buffered Saline
HEPES	N-(2-Hydroxyethyl) piperazine-N'-2-ethanesulfonic acid
Hsp70	Heat-shock Protein 70
IgG	Immunoglobulin G
IMAC	Immobilized Metal Affinity Chromatography
IPTG	Isopropyl B-D-thiogalactopyranoside
ITC	Isothermal Titration Calorimetry

ITI	Immune Tolerance Induction
K_a	Equilibrium association rate constant
K_D	Equilibrium dissociation rate constant
LB	Lysogeny Broth
mAb	Monoclonal antibody
MES	2-(N-morpholino) ethanesulfonic acid
MWCO	Molecular weight cut-off
OD	Optical density
PEG	Polyethylene glycol
pI	Isoelectric point
PMSF	Phenylmethylsulfonyl Fluoride
PS	Phosphatidylserine
rFVIII	Recombinant FVIII
rFVIIa	Recombinant activated FVII
RT	Room temperature
SAXS	Small Angle X-ray Scattering
SDS-PAGE	Sodium Dodecyl Sulfate – Polyacrylamide Gel Electrophoresis
SEC	Size Exclusion Chromatography
SPR	Surface Plasmon Resonance

TBS	Tris-buffered Saline
TEM	Transmission Electron Microscope
TEV	Tobacco Etch Virus
TF	Tissue Factor
TFPI	Tissue Factor Protein Inhibitor
Tris-HCl	tris(hydroxymethyl)aminomethane hydrochloride
v/v	volume/volume
VH	Heavy-chain variable domain
VL	Light-chain variable domain
Vmax	Maximum velocity of an enzymatic reaction
vWF	von Willebrand Factor
w/v	weight/volume
WT	Wild-type
Xase	Tenase

Introduction

Hemostasis is a physiological process employed at the site of an injury in order to cease bleeding and simultaneously maintain normal blood flow throughout the rest of the body.[1] Hemostasis is separated into two distinct components that work in tandem to form clots: primary and secondary hemostasis. Primary hemostasis involves platelet plug formation and platelet aggregation. Over the course of primary hemostasis, platelets are activated and subsequently adhere to the site of injury to seal it.[1] The work presented in this thesis concerns secondary hemostasis, which results in a cross-linked fibrin mesh that serves to stabilize the platelet plug generated from primary hemostasis.[2] The fibrin responsible for this mesh is generated through the proteolytic coagulation cascade carried out by a variety of blood coagulation factors.[1] To achieve timely completion of the cascade, each coagulation factor is essential. Deficiency or loss of function in certain proteins involved in this process leads to a variety of different bleeding disorders such as hemophilia A/B and Von Willebrand disease. Deficiency or loss of function of coagulation factor eight (FVIII) gives rise to hemophilia A, resulting in a 100,000 fold slowing of blood clot formation. This rate of depreciation can be attributed to FVIII's inability to function as a coenzyme for a crucial part of the cascade. Patients with hemophilia A are given frequent injections of FVIII into their bloodstream so that the cascade may continue, however significant complications are associated with this process. The most pressing issue is the development of anti-FVIII inhibitory antibodies by the patient rendering the injected FVIII physiologically useless. The work outlined in this thesis discusses the interactions between FVIII and these antibodies and the different ways FVIII can mechanistically be inactivated by them.

Primary Hemostasis

Primary hemostasis involves the formation of a soft plug at the site of injury that serves as the first response to vascular injury. This action is carried out by activated platelets that rapidly adhere and aggregate at the injury in an attempt to stop bleeding.[1] Platelets are small fragments originating from

megakaryocytes, or large polyploid blood cells in the bone marrow.[1,2] They are present in quantities of 150 to 400 million and typically circulate for 10 days prior to clearance.[2] The platelet aggregate formed during this process provides the base for the cross-linked fibrin clot formed in secondary hemostasis.[1]

Platelet Adhesion

Platelets do not aggregate or adhere to surfaces under normal blood flow.[2] However upon injury, they are exposed to the subendothelial matrix and adhesion begins. Adhesion is mediated by von Willebrand factor (vWF), a large multimeric protein secreted from endothelial cells.[2] vWF is always present in its immobilized state in the subendothelial matrix as well as its soluble state in plasma.[2] The key platelet receptors with regards to adhesion are known as glycoprotein VI (GPVI) and glycoprotein IX-V (GPIb-IX-V).[1,2] Upon injury, GPIb-IX-V binds to vWF. Upon adherence to the injured area, platelets undergo a conformational change to a pseudopodal or arm-like shape in order to activate the GVPI collagen receptors on their membrane surfaces.[1,2] As this occurs, they release ADP, platelet activating factors, serotonin, and thromboxane A2 all to promote aggregation.[1,2]

Platelet Aggregation

Once activated, the GpIIbIIIa platelet receptor is triggered allowing the platelets to adopt a pseudopodal shape in which they extend and clump with other activated platelets.[1,2] As the platelets clump, a soft plug at the site of injury is formed.[1,2] This plug forms the base for what will eventually become a stable fibrin clot following completion of the coagulation cascade during secondary hemostasis.

Secondary Hemostasis

Secondary hemostasis results in the cleavage of soluble fibrinogen to insoluble fibrin by thrombin to form a fibrin clot following the blood coagulation cascade.[2] This fibrin is a mesh formed in

and around the soft plug generated from primary hemostasis to stabilize and strengthen the clot.[2] This process occurs in tandem with primary hemostasis.[2]

The Blood Coagulation Cascade

The coagulation cascade is initiated through two different pathways: the extrinsic pathway and the intrinsic pathway.[3] As the cascade proceeds, the intrinsic and extrinsic pathways ultimately converge into the common pathway.[3] The common pathway, once completed, results in the formation of a clot. Until recently, the notion of intrinsic and extrinsic pathways was thought to be sufficient for describing this process. A recently proposed model comprised of initiation, amplification, and propagation will be discussed in this section to account for the dynamic nature of the cascade. Each coagulation factor involved in the cascade exists as a zymogen as they are inactive until they are proteolytically activated.[4] For the cascade to work as intended, each factor is crucial and even the smallest deficiency in any of their functionalities can have drastic effects on the efficiency of the cascade. For example, factor IV (calcium ions) is essential for every single step of the pathway as it is required to bind to lipid surfaces, on which the majority of the cascade proceeds.[3] The required proteins and coagulation factors to carry out the cascade are detailed below in Table 1.

Table 1. Blood coagulation factors and other proteins contributing to the blood coagulation cascade.[5]

Coagulation Factor or Associated Protein	Role in Cascade
Factor I (fibrinogen)	Forms clot, precursor to fibrin
Factor II (prothrombin)	When activated, activates factors I, V, X, VII, VIII, XI, XIII, protein C, and platelets
Factor III (tissue factor)	FVIIa cofactor
Factor IV (Calcium ions)	Facilitates coagulation factor binding to phospholipid platelet surfaces
Factor V	FX cofactor, forms prothrombinase complex with FX
Factor VII	Activates FIX and FX
Factor VIII	Cofactor for FIX, forms intrinsic tenase complex when bound
Factor IX	Forms intrinsic tenase complex with FVIII, activates FX
Factor X	Activates prothrombin, forms prothrombinase complex with FV
Factor XI	Activates FIX
Factor XII	Activates FXI, FVII, and prekallikrein
Factor XIII	Crosslinks fibrin
von Willebrand Factor	Carrier protein for FVIII which prevents premature clearance of FVIII, regulates platelet adhesion
Protein C	Neutralizes FVa and FVIIIa
Protein S	Activated Protein C cofactor

Initiation

The primary initiator protein of the coagulation cascade is known as tissue factor (TF), which is localized outside the vascular system to prevent initiation under normal conditions.[4] Once an injury occurs and a cell bearing TF comes into contact with flowing blood, activated factor 7 (FVIIa) immediately binds exposed TF.[4] This is possible because FVII is the only coagulation factor present in its activated state in blood, although only 1% of all FVII in blood is thought to be activated.[4] The initial TF:FVIIa complex acts to activate additional zymogenic FVII to increase TF:FVII activity.[4] This complex

goes on to activate factor 9 (FIX) and factor 10 (FX).[4] FIXa then slowly activates factor 5 (FV) and subsequently forms the prothrombinase complex, responsible for cleaving prothrombin to produce small amounts of thrombin.[4] Excess FXa that dissociates from the surface of the TF-bearing cell is instantly neutralized by either antithrombin (AT) or tissue factor protein inhibitor (TFPI).[4]

Amplification

At this point, a sufficient amount of thrombin has been generated and is available outside of the TF-bearing cell. This thrombin comes into contact with platelets at the site of injury and subsequently helps activate them.[4] This interaction promotes aggregation of the platelets for soft plug formation alongside the granular fuel released from platelets upon conformational change.[4] Additional generated thrombin goes on to cleave factor 11 (FXI) to FXIa and FV to FVa on the platelet surface.[4] Factor 8 (FVIII) is also cleaved from its carrier protein vWF by thrombin. Cleaved vWF generated from this process then serves to regulate platelet aggregation.[4] The free FVIII is immediately activated by thrombin once it is released from vWF.[4]

Propagation

As platelet aggregation occurs, sufficient platelet surface space is now available for FIXa produced during initiation to bind to FVIIIa to form the intrinsic tenase complex.[4] The intrinsic tenase complex rapidly activates additional FX through cleavage on the platelet surface which then binds to FVa to cleave more prothrombin into thrombin.[4] The thrombin from this step is in excess, and goes on to cleave fibrinopeptide A from fibrinogen.[4] Due to the sheer speed of this thrombin generation and following fibrinogen production, a critical mass of fibrin is produced which polymerizes into a cross-linked fibrin clot to fully seal the injury.[4]

Blood Coagulation Factor VIII

FVIII is a 2332 residue glycoprotein that functions as an essential cofactor for FIXa in the coagulation cascade.[6] Although it is a cofactor, FXa production is slowed 100,000 fold if FVIII is absent or non-functional and thus slows the overall clotting process drastically.[6] FVIII is synthesized from the *f8* gene on the tip of the long arm of the X chromosome and spans approximately 186 kbp.[7] It consists of 26 exons and 26 introns and has a coding sequence length of 9 kbp.[7] It is expressed primarily in liver cells, specifically liver sinusoidal cells.[7] However significant amounts of FVIII have also been observed in hepatocytes and resident macrophages of liver sinusoidal cells (Kupffer cells).[7] The FVIII polypeptide has the domain organization A1-A2-B-A3-C1-C2 with the A domains and C domains sharing 30% and 37% homology respectively (Figure 1, Figure 2).[7,8] The B domain has no known homologues.[8]

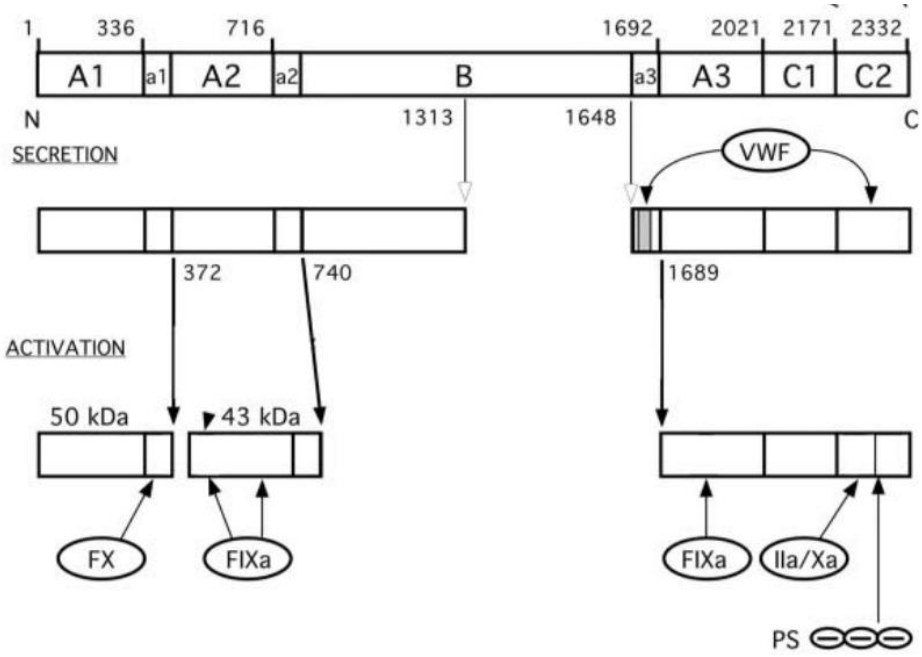

Figure 1. Schematic view of FVIII domain organization detailing cleavage sites for activation and secretion. Sites of relevant interactions with other coagulation factors and platelet surfaces (PS) are also pictured.[10]

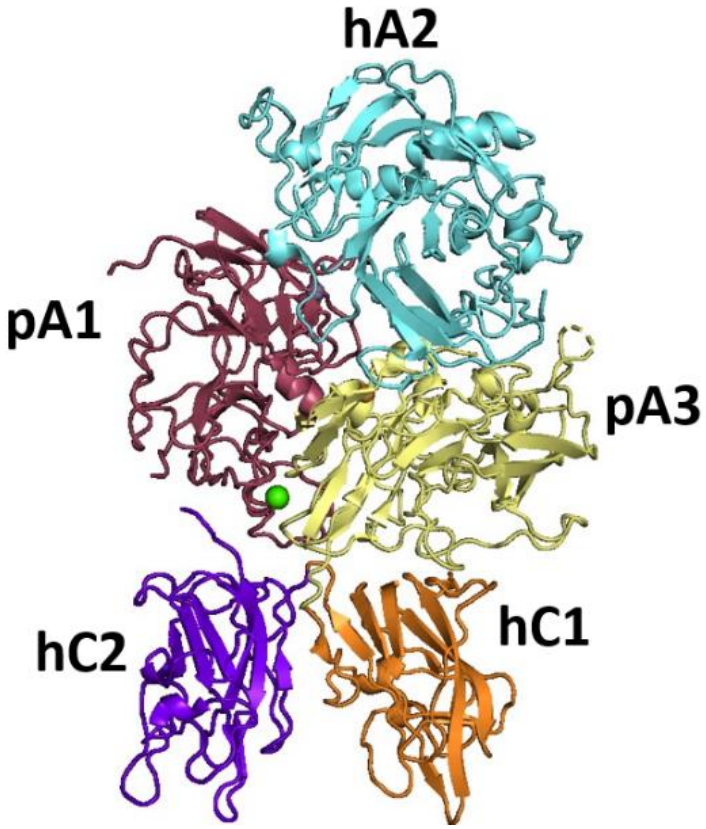

Figure 2. Crystal structure of BDD (B-domain deleted) chimeric human/porcine FVIII construct Et3i. (PDB: 6MF2)

Instantly upon release into circulation, FVIII forms a tight noncovalent complex with carrier protein vWF which binds all domains besides the B domain.[9] This interaction with vWF ensures that FVIII is not prematurely activated or cleared and prevents FIXa or phospholipid binding.[9] Upon proteolytic activation by thrombin, FVIII dissociates from vWF, loses its B domain, and conformationally shifts to a shape capable of binding FIXa and FX on activated platelet surfaces.[9]

Hemophilia A

Hemophilia A is an X-linked bleeding disorder caused by mutations in the *f8* gene resulting in a deficiency or lack of functional FVIII in a patient's bloodstream.[11] Individuals with this disorder suffer from bleeding episodes in which their body cannot form blood clots fast enough to seal injuries. The bleeding sites for these episodes are usually in their joints, muscles, or soft tissues.[11] Hemophilia A

affects 1:5000-10,000 newborn males worldwide and is the most common bleeding disorder in men.[11] Severity of hemophilia A can vary on a patient-to-patient basis. Severity is categorized by the amount of residual FVIII in their blood. Mild cases have 5-40% FVIII in their blood relative to normal FVIII levels, moderate cases have 1-5%, and severe cases have less than 1%.[11]

Although less common, genetically uninherited acquired hemophilia A also exists. This condition stems from the spontaneous development of autoantibodies capable of neutralizing FVIII in previously healthy individuals.[12] This condition reportedly only affects 1 in 1 million people per year, and is rarer than its inherited counterpart.[12] This ratio is thought to be lower as it is probable that some cases remain undiagnosed due to their lack of severity and likely lack of treatment.[12] Acquired hemophilia A is predominantly observed in elderly patients and post-partem women.[12] The exact cause of this condition is yet to be determined, but in 50% of cases, some researchers believe that underlying diseases may play a role in the immune system's generation of antibodies against FVIII. These diseases include lupus, rheumatoid arthritis, multiple sclerosis, Sjogren's syndrome, temporal arteritis, inflammatory bowel disease, infection, diabetes, hematological cancer, and respiratory and dermatological diseases.[12] For the other 50% of patients, development of acquired Hemophilia A is thought to be idiopathic.[12]

Hemophilia A Treatment

Currently, the most common treatment for hemophilia A is FVIII infusion therapy. In this treatment, hemophiliacs are injected with FVIII in the form of plasma, protein concentrates, or blood.[13] Due to the 8-12 hour half-life of FVIII in the body, patients must receive prophylactic infusions two to three times per week for their entire life.[13] This process can cost $200,000-$300,000 annually, placing a severe financial burden on patients who struggle to cover treatment expenses.[13] A variety of FVIII constructs with up to two-fold longer half-lives than human FVIII have been developed to reduce the frequency of infusions, but treatment with these products typically ends up being more expensive than

the more frequent FVIII infusion therapy.[12] In general, even the primary and best treatments for hemophilia A have significant limitations, necessitating the need for more efficient treatment options.

Development of Inhibitory Antibodies

The most common issue facing FVIII infusion therapy is the development of anti-FVIII inhibitory antibodies by the patient's immune system. These antibodies drastically reduce the treatment's efficacy as the majority of the injected FVIII is rendered useless once the antibodies bind to it. Anti-FVIII antibodies are present in approximately 30% of severe hemophilia A patients and appear within 20-50 days following treatment.[13] Patients possessing these inhibitors experience a decreased quality of life and higher mortality relative to those lacking them.[14] Additionally, the cost of FVIII infusion therapy plus inhibitor treatment is the highest reported for a chronic disease.[13]

Immune tolerance induction (ITI) is the only available inhibitor-reduction treatment for hemophiliacs that has proven successful. The exact mechanism of this treatment is unknown, but the underlying notion behind it is that the that introduction of FVIII to the body under non-inflammatory conditions will lead to a tolerance for FVIII.[14] This results in a down-regulation of the immune response to injected FVIII and a lower likelihood of inhibitor development.[14] Unfortunately, this treatment is only successful in 60-80% of cases and often takes years to build the required tolerance.[14] It also costs around $850,000 a year per patient.[14]

Modified FVIII Replacements: Porcine FVIII Approaches

To mitigate the issues surrounding FVIII infusion therapy and increase its efficacy, various FVIII constructs have been produced possessing longer half-lives and greater stability than native human FVIII. From the mid-20th to the early 21st century, plasma-derived porcine FVIII (pd-pFVIII) played an important role in hemophilia A treatment. In the early 1980s, a pd-pFVIII concentrate was released that successfully increased FVIII procoagulant activity to circulating levels in high-titer inhibitor patients. It

displayed a longer half-life and lower immunogenicity than human FVIII, with low-titer inhibitor patients not developing any more inhibitors than were previously present.[15] Following the epidemic in the late 1970s to the early 1980s stemming from the transmission of blood-borne viruses such as hepatitis B/C and human immunodeficiency virus, the necessity for safer hemophilia A treatments catalyzed the development of recombinant FVIII products.[16] Revolutionizing hemophilia A treatments, recombinant FVIII products overcome the limited availability of plasma-derived products to a significant degree, although recombinant FVIII production is still a difficult and laborious process.[16] Obizur (Takeda®), is a recombinant B-domain-deleted (BDD) pFVIII construct produced using baby hamster kidney cells (BHK) in serum/vWF-free media.[15] Plasma samples from inherited hemophilia A patients dosed with Obizur show increased levels of thrombin generation and clot formation. Recombinant pFVIII also has greater bioavailability than pd-pFVIII, displaying its usefulness as an alternative to plasma-derived treatments.[16]

During ITI campaigns, large amounts of FVIII for long stretches of time are required to achieve FVIII tolerance and reduce inhibitor titers.[14] Noting this, Expression Therapeutics (Emory University) developed the BDD human/porcine chimeric FVIII construct "Et3i". This construct contains porcine A1/A3 domains and expresses roughly 5-fold higher than recombinant human FVIII (rhFVIII) while displaying comparable procoagulant activity.[17] Although not presently approved as a viable therapeutic for hemophilia A treatment, the gifting of Et3i to the Spiegel lab by the Lollar lab at Emory University has proven indispensable in expanding our structural knowledge of FVIII's interactions with inhibitory antibodies and other cascade-related processes.

Modified FVIII Replacements: Extended Half-life Approaches

To reduce frequency of FVIII infusions during hemophilia A treatment, several efforts have been made to extend the half-life of injected FVIII. Conjugation of polyethylene glycol (PEG) to therapeutic molecules has previously proven successful in extending their half-lives. This approach was applied to

hemophilia A treatment through the development of B-Domain Selectively PEGylated rhFVIII (Adynovate, Shire Pharmaceuticals®). Adynovate extends the half-life of rhFVIII through controlled PEGylation in which 60% of PEG chains are covalently bound to the B-domain.[18] As the B-domain is largely removed from FVIII during thrombin activation, the B-domain is an ideal candidate for PEGylation. Additionally, PEGylation of this region reduces steric interferences in FVIII's binding of vWF, platelet membranes, and FIXa/FX that could arise from uncontrolled PEGylation of FVIII. When compared to rhFVIII, Adynovate shows a relative half-life increase of 1.5x.[18]

FVIII half-life extension has also been achieved through the fusion of FVIII with the Fc region of an immunoglobulin molecule known to possess a long half-life. Immunoglobulins and albumin make up upwards of 90% of serum proteins, and maintain their plasma concentration through a balancing of synthesis, degradation, and recycling pathways. One key recycling pathway associated with these proteins is the pathway involving the neonatal Fc receptor (FcRn) expressed on endothelial cells.[19] The key characteristics of this pathway are the uptake of these proteins by endocytosis and delivery to endosomes. Both immunoglobulin and albumin molecules bind to FcRn with high affinity and are protected from degradation as a result. This process was taken advantage of in the development of Eloctate (Bioverativ Inc.®), a fusion of BDD rFVIII to an Fc dimer which has a half-life ~1.5x that of rFVIII.[19]

Bypassing Agents: rFVIIa and aPCC Therapy

Aside from FVIII infusion therapy, a variety of other treatment options are available for Hemophilia A patients. A common approach to the treatment of hemophilia A patients possessing inhibitory antibodies is the use of bypassing agents. Bypassing agents offer a unique approach to hemostasis through their augmentation of clotting capabilities without administration of FVIII. These agents include activated prothrombin complex concentrates (aPCC), recombinant activated factor seven (rFVIIa, Novo Nordisk®), and Emicizumab (Roche®). Both rFVIIa and aPCC treatments facilitate

hemostasis through thrombin generation in the absence of FVIII at the site of injury.[20] The mechanisms of action for these treatments are not yet fully understood, but Factor Eight Inhibitor Bypassing Activity (FEIBA, Baxter®), targets the prothrombinase complex. In the prothrombinase complex, FXa converts prothrombin to thrombin while bound to phospholipids.[20] Presently, FEIBA is the only aPCC treatment available in the United States and exists as a cocktail of coagulation factors II, IX, X and VIIa.[21] Secondary prophylaxis, also known as rFVIIa infusion, has proven beneficial for hemophilia A patients with inhibitors. Treatment with rFVIIa stimulates the production of increased amounts of extrinsic pathway TF:rFVIIa activated FX in order to maintain clotting capabilities in high-inhibitor environments. This treatment also works to minimize joint bleeding, and in turn the risk of bleeding-induced arthropathy.[22]

Bypassing Agents: Emicizumab

Emicizumab is a bispecific mAb of the isotype IgG4 that mimics FVIIIa function through its bridging of FIXa and FX to catalyze FX activation. To facilitate this process, Emicizumab is designed to recognize FIX/FIXa with one Fab arm and FX/FXa with the other. This therapeutic has a significant advantage over FVIII infusion therapy in that inhibitory antibodies generated by the patient immune system in response to FVIII's presence fail to recognize it.[13] However, this is not to say that Emicizumab does not possess a number of disadvantages as well. As previously mentioned, Emicizumab simulates FVIIIa, meaning that it does not require activation by thrombin and is always active. This routinely interferes with clotting assays such as activated plasma thromboplastin time (aPTT) where Emicizumab's presence leads to a higher observed coagulation rate due to the skipping of the time typically required to generate FVIIIa in the coagulation cascade. Underestimation of FVIII inhibitor titers during the Bethesda assay is another consequence of this therapeutic as Emicizumab retains its activity in the presence of FVIII inhibitors.[13]

Unlike FVIIIa, Emicizumab is incapable of binding to phospholipids. This means that since the activation of FX through the FVIIIa:FIXa complex takes place on negatively-charged phospholipids, Emicizumab's procoagulant activity is still phospholipid-dependent. As a result, Emicizumab's activity is most likely limited to the site of injury, where exposed negatively-charged phosphatidylserine (PS) binds the Gla domains of FIX and FX. Despite these limitations, Emicizumab is a licensed treatment for hemophilia A patients both possessing and lacking inhibitors and has seen efficacious use as a treatment option.[13]

Gene Therapy

Given the nature of current hemophilia A treatment, which involves lifelong infusions of various products, gene therapy as a treatment option presents the potential of long-term FVIII expression in hemophiliacs and a resulting increase in quality of life. Until very recently, there were no FDA-approved gene therapy treatments for hemophilia A. But on June 29th, 2023, Roctavian (BioMarin Pharmaceutical Inc.®) was approved for use in hemophilia A treatment for individuals lacking pre-existing inhibitors. Roctavian is an adeno-associated virus vector-based gene therapy administered as a single-dose intravenous infusion. The viral vector carries a gene coding for FVIII and is subsequently expressed in liver cells following infusion. Infusion with Roctavian can cause mild changes in liver function, headache, nausea, vomiting, fatigue, abdominal pain, and even increased FVIII levels exceeding normal limits.[23] Although the long-awaited arrival of gene therapy has finally come, this treatment is not yet a true solution to hemophilia A. Since this treatment is only approved for individuals lacking inhibitors, the 30% of severe hemophilia A patients who suffer from inhibitor development cannot receive gene therapy. Additionally, Roctavian administration is limited to patients over the age of 18, meaning that minor hemophiliacs will still require traditional treatments.[23]

FVIII Inhibitory Antibodies

FVIII inhibitory antibodies take the form of immunoglobulin G's (IgG), the most common type of antibody in human serum. In the case of FVIII inhibitors, FVIII is treated as an antigen by the patient's body and when introduced triggers B-cells to secrete IgGs to fight it off.[24] They are composed of four polypeptide chains, consisting of two identical 50 kDa heavy chains, and two identical 25 kDa light chains which are all linked together by inter-chain disulfide bonds (Figure 3). The heavy chains consist of N-terminal variable domains (VH) and three constant domains known as CH1, CH2, and CH3. They have a flexible hinge region as well located between the CH1 and CH2 domains. The light chains are arranged in a similar fashion, consisting of an N-terminal variable domain (VL) and a constant domain (CL).[24] The light chain associates with the VH and CH1 domains of the heavy chain to form the Fab region responsible for antigen binding.[15] The lower hinge region and the CH2/CH3 domain is known as the Fc or "fragment crystallizable" region which plays no part in antigen binding.[24]

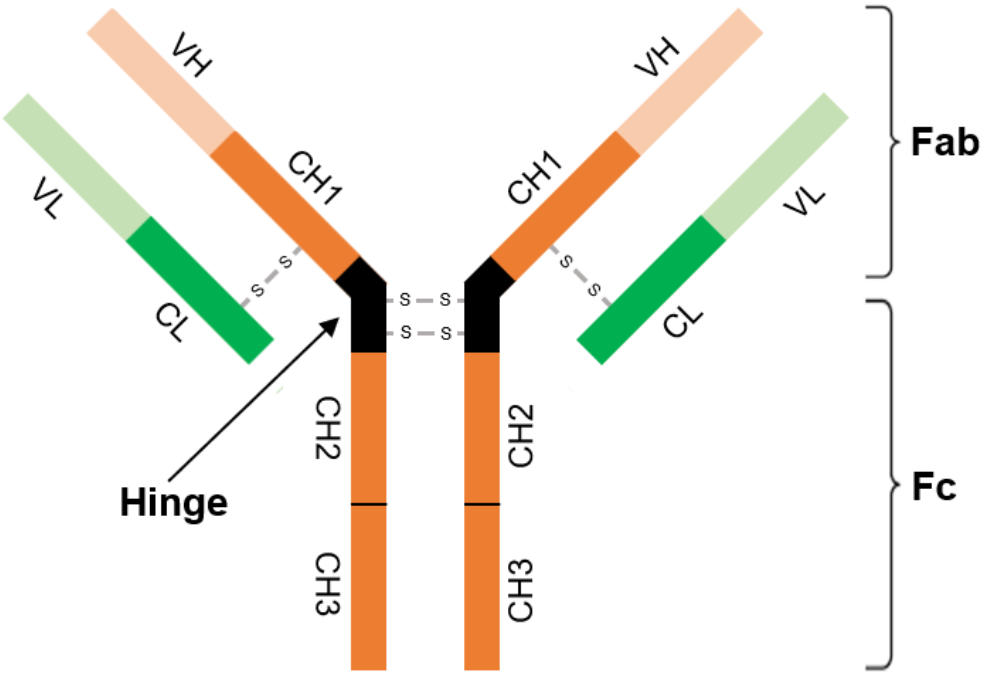

Figure 3. General structure of a monoclonal antibody.

Anti-A2 Antibodies of Study

With regards to the structure of FVIII, the A2, A3-C1 and C2 domains are the most immunogenic although antibodies exist for all domains. When an antibody binds to FVIII, FVIII is inhibited sterically from interacting with its various key binding partners in the coagulation cascade. The A2 domain is the site at which FIX associates with FVIII to form the intrinsic tenase complex.[25] Should an antibody be present on the A2 domain, FIX can no longer form the tenase complex and the cascade is drastically slowed. The C1 and C2 domains are involved in lipid binding to platelet surfaces as well as binding to vWF, so these interactions are also blocked if antibodies are present on these domains.[25]

Anti-FVIII antibodies are classified based on the kinetics by which they inhibit FVIII as well as the extent of inhibition. Type I inhibitors follow a dose-dependent linear pattern (second-order kinetics) and completely inactivate FVIII. Type II inhibitors do not completely inactivate FVIII and have complex kinetics.[25] Anti-A2 antibodies are grouped into group A, AB, B, BCD, C, D, DE, and E based upon epitope overlap on B-cells.[26] Group A antibodies noncompetitively inhibit at the epitope range of Arg484-Ile508 on FVIII which halts the formation of the intrinsic tenase complex. Group B and C antibodies display very little inhibitory activity, whereas group D and E antibodies inhibit thrombin cleavage of FVIII preventing its activation.[26]

Six unique anti-A2 antibodies will be explored throughout the work in this thesis. Group A inhibitor 4A4, group B inhibitor 4F4, and group E inhibitors 4C7 and 1D4. The groups to which mAbs 2-101 and NB11B2 can be classified as are unknown. 4A4, NB11B2, 4F4, and 1D4 are all type I inhibitors fully inactivating FVIII. 4C7 is non-inhibitory, while 2-101 is type II, incompletely inactivating FVIII.[26,27] When measuring extent of inhibition, Bethesda units (BU) are used. One BU per milliliter is defined as the dilution of inhibitor that produces 50% inhibition of FVIII activity.[26] The types, groups, BU titer, and epitopes of each antibody are listed below in Table 2.

Table 2. Anti-A2 domain antibodies of study and their respective properties.[26,27]

Antibody of Study	Group	Type	BU/mg IgG	Epitope
4A4	A	I	40,000	Asp^{403}-His^{444}
1D4	E	I	7,000	Glu^{604}-Arg^{740}
4F4	B	I	330	Indeterminate
4C7	E	Non-inhibitory	<1	Indeterminate
2-101	Unknown	II	11,000	His^{444}-Arg^{541}
NB11B2	Unknown	I	11.964	Arg^{484}-Phe^{509}

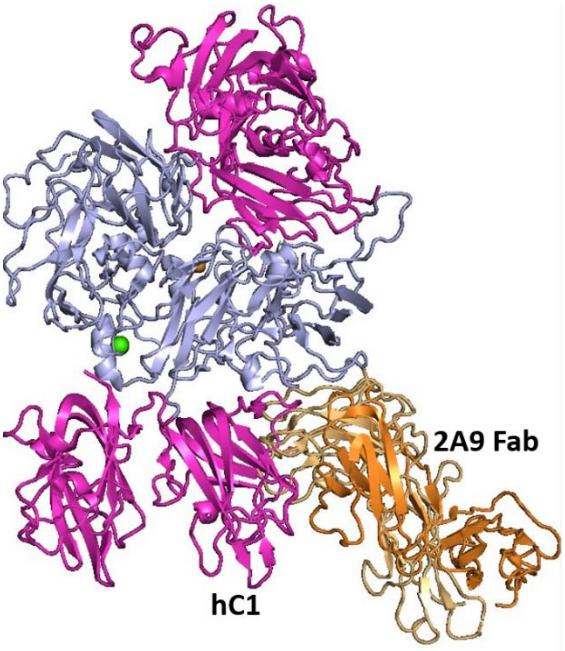

Figure 4. B-domain deleted human/porcine chimeric FVIII construct Et3i bound to anti-C1 inhibitor 2A9. PDB: 7K66

As previously mentioned, severe hemophilia A patients who develop inhibitory antibodies while receiving FVIII infusion therapy usually develop inhibitors that bind to either the A2 or C2 domains. But in recent years, inhibitors binding to the FVIII C1 domain have been identified that have overlapping epitopes with sites on FVIII involved in platelet and vWF binding.[28] These mAbs can be grouped into either group A or B. Group A inhibitors, while displaying high binding affinity for FVIII, do not significantly impact FVIII procoagulant activity and tend to poorly inhibit platelet binding. They also do not consistently block FVIII's binding to vWF.[28] Group B inhibitors have a much more pronounced effect on FVIII's function. They have been shown to potently inhibit FVIII procoagulant activity, binding to vWF/platelets, FVIIIa's role in the formation of the intrinsic tenase complex, uptake in

dendritic cells, and thrombin generation in plasma.[28] NB2E9, a recombinant version of mAb LE2E9, belongs to group A and decreases FVIII activity by 80-90% through binding interference with vWF. Anti-C1 inhibitor 2A9, whose FVIII-bound structure was solved previously in the Spiegel lab, has a largely overlapping epitope with LE2E9 and similarly interferes with vWF binding (Figure 4).[29]

LE2E9 was originally isolated from a patient with mild hemophilia A receiving injections of recombinant FVIII.[29] Upon receiving these injections, the patient developed a high-titer inhibitor but FVIII levels did not change despite the inhibitor developing. This patient and their brother both carried the C1 domain mutation R2150H, and both exhibited unchanging levels of FVIII following rFVIII administration. It was therefore concluded and later confirmed that the specificity of this inhibitor was restricted to wildtype FVIII.[30]

LE2E9 is unique to most monoclonal antibodies in that it contains a Asn-linked glycosylation site on one of its variable region heavy chains. The removal of this glycosylation reduced LE2E9 FVIII inhibition to 40% from its original 80%, illustrating the important role this glycan plays in FVIII inhibition.[31] This removal also resulted in the Vmax of the formation of the Xase complex slowing by 55% rather than 77% as reported with LE2E9 in its native glycosylated state.[32] The LE2E9 construct lacking this glycan also failed to disrupt FVIII binding to vWF.[31] Following these observations, a mutant LE2E9 lacking the glycan was created and termed “TB402”. TB402 was originally developed as an antithrombotic used for postoperative thromboprophylaxis to prevent excess bleeding. TB402 slows FVIII activity to 50% and despite some success in phase III clinical trials, it has not achieved widespread use beyond this.[29] Solving the structure of FVIII bound to NB2E9 may provide insight into the variety of novel mechanistic behaviors displayed by this mAb when reducing FVIII activity.

Structural Studies of FVIII:Inhibitor Complexes

When designing therapeutics for hemophilia A treatment, structural information about how antibodies interact with each domain has proven indispensable. Exact epitope location is the most valuable tool in learning how each inhibitor inactivates FVIII. Previous work in the Spiegel lab at WWU has resulted in the structural characterization of BDD FVIII bound to anti-C2 domain antibody G99 and anti-C1 domain antibody 2A9 (Figure 4). This work was accomplished via X-ray crystallography, in which protein crystals are grown, shot with X-rays, and have their structure modeled based upon the diffraction pattern they exhibit.[33] To grow crystals, proteins are typically concentrated as highly as possible and placed into conditions promoting supersaturation. Supersaturation is the state at which proteins are nearly insoluble, and form crystals in solution rather than simply precipitating out. This is accomplished through the use of precipitants such as PEG, buffers at different pH values, salts, and a variety of other potential materials. These materials include regents such as silica/paraffin oil, which slow the rate of vapor diffusion and potentially increase crystal size. Protein crystallization is typically performed through hanging-drop vapor diffusion, which involves a small amount of protein solution mixed with reservoir solution on a cover slip hanging above a reservoir of solution.[33] In this technique, the pressure of water around the drop is greater than the pressure around the reservoir, which is typically 200x the size of the drop. The pressure gradient in the space between the drop and the reservoir results in a loss of water from the drop which works to precipitate the protein out of solution into its crystalline form. If this process occurs too quickly, the protein will precipitate out of solution without forming crystals.[33]

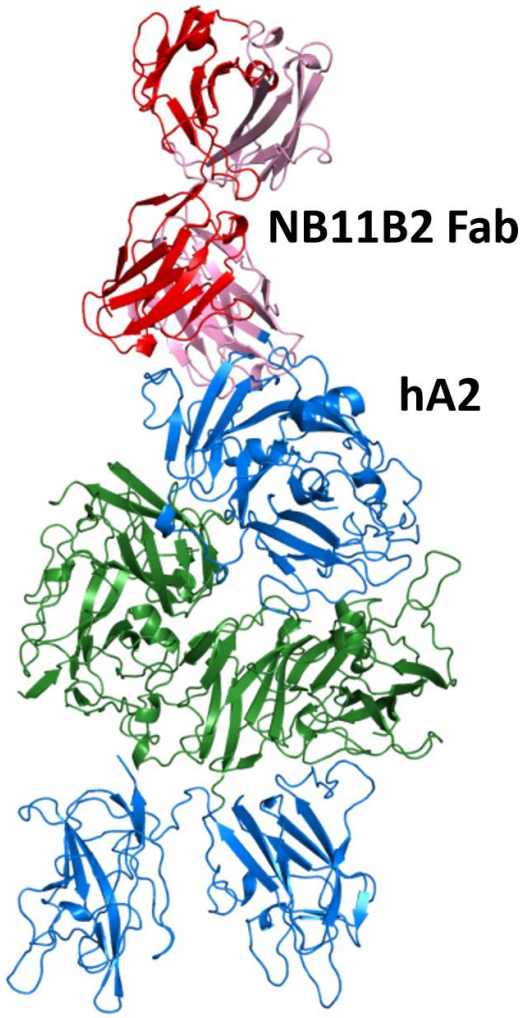

Figure 5. Cryo-EM structure of patient-derived anti-A2 domain FVIII inhibitor NB11B2 in complex with BDD-FVIII construct Et3i. (Unpublished data, K. Childers)

In recent years, cryogenic electron microscopy (Cryo-EM) has seen major advances in image recording and processing software allowing it to rival X-ray crystallography as a method of determining high-resolution three-dimensional models of macromolecular assemblies. This technique has many advantages compared to X-ray crystallography, primary among these is that no crystallization is required, which is the typical rate-limiting step of crystal structure generation. Far less sample is required for Cryo-EM experiments, with concentrations ranging from 10 mg/mL to 0.01 mg/mL depending on the sample's characteristics.[34] K. Childers in the Spiegel lab has so far managed to produce three unique FVIII-inhibitor structures using Cryo-EM, including the structure of Et3i bound to anti-A2 domain inhibitor NB11B2 (Figure 5).

To perform a Cryo-EM experiment, the sample is first diluted to the desired concentration and subsequently applied to a charged EM grid. As the protein sample is applied to the grid, the sample particles find their way into the fine holes located within the grid's surface. After using filter paper to remove excess protein stock from the grid, the grid is plunged into liquid ethane cooled by liquid nitrogen and flash-frozen. This technique allows for the freezing of the sample in its native state while maintaining a protective layer of ice encompassing the sample.[34] This ice layer must be sufficiently thin so that particle contrast upon data collection will not be too low. Following grid preparation, the grid is

loaded into a transmission electron microscope (TEM) designed to maintain liquid nitrogen temperatures during data collection.[34] The TEM then bombards the grid with electrons and images are formed as the electrons interact with the sample. Once all images have been collected, the user must sort through them in order to identify particles of interest. An initial 3-D map can then be generated using 2-D projections as a starting point. From this point, the structure can be modeled into the map using the sequence of the sample.[34]

Small-angle X-ray scattering (SAXS) has also been employed in lieu of crystallization and provides a low-resolution molecular envelope that can be used to model in known structures of antibodies and antigens separately to generate predictive models of their bound complex state. In a SAXS experiment, proteins are completely in solution, contrary to X-ray crystallography. The proteins are exposed to X-ray radiation of a specific wavelength which scatters between 0 and 5 degrees to produce a spatially averaged intensity distribution that a molecular envelope can eventually be generated from.[35] Although low-resolution, this technique is an attractive alternative to X-ray crystallography specifically in the case of FVIII-antibody complexes as they can be very difficult to crystallize due to their large size, glycosylation, and general lack of symmetry.

Proposed Cooperative Binding of FVIII by Inhibitors

Upon the structural determination of the human C2 domain of FVIII in complex with G99 and 3E6 Fab fragments, evidence was gathered suggesting the cooperative binding of the C2 domain by these two inhibitory antibodies (Figure 6). G99 is known as a non-classical inhibitor, in that its binding prevents FVIII from being activated by FXa or thrombin. This results in an inability to dissociate from vWF.[36] 3E6 is a classical inhibitor, blocking the FVIII C2 domain from associating with platelet surfaces and/or vWF.[37]

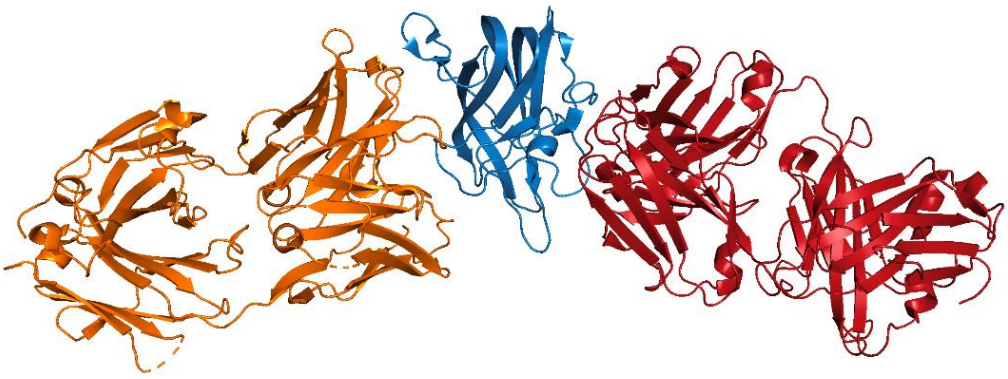

Figure 6. X-ray crystal structure of the human C2 Domain of FVIII (blue) bound to inhibitor Fab fragments G99 (orange) and 3E6 (red). PDB: 4KI5.

As shown in Figure 6, G99 and 3E6 bind to opposite sides of the C2 domain. 3E6 binds to residues including Lys2183, Asp2187, and Arg2215, which are likely involved in vWF binding. G99 forms contacts with Glu2228 and Trp2229, which predictively interact with FIXa. Additionally, the hydrophobic region containing Leu2261, Ser2263, and Phe2265 is buried. This region has previously been shown to bind to FXa.[36]

Upon G99's binding of C2, B-factor analysis of the crystal structure of Et3i:G99 in the epitope range of residues 2269-2282 shows a 37.9% decrease in B-factor value when compared to those of free Et3i.[36] In short, B-factors can be defined as the relative level of rigidity in a given region, with low B-factor values indicating rigidity and high B-factor values indicating flexibility.[36] From this analysis, it can be said that G99's binding works to rigidify the C2 domain. In the Et3i:G99 structure, the region spanning residues 2202-2215, or the 3E6 epitope, showed a 18% decrease in B-factor value, indicating rigidification of this area as well.[36] From this set of analyses, it was proposed that the binding of G99 to C2 lowers the entropic cost of 3E6 binding simultaneously, displaying positive cooperativity between the two inhibitors.

Isothermal titration calorimetry (ITC), a method to determining the thermodynamics of a given protein-macromolecule interaction, is commonly employed to assess cooperativity between two ligands capable of binding to the same macromolecule. The entropy (ΔS), enthalpy (ΔH), stoichiometric ratio

between ligand and macromolecule (N), association constant (K), and the change in free energy (ΔG) can all be calculated from a single ITC experiment for a given system of binding partners. Most calorimeters used for ITC involve three central components. These are a reference cell filled with buffer matching the buffer used for the binding experiment, a sample cell, and an injection syringe.[38] In a typical ITC experiment, the ligand is titrated in small portions from the syringe into the sample cell containing the macromolecule. As the titration takes place and binding events occur, the reference cell acts to normalize the ΔH as heat gets released/absorbed. In an exothermic reaction, the temperature of the system increases and the instrument reduces power in order to maintain a constant baseline signal between the sample and reference cells.[38] Each binding event produces a peak on what is called a thermogram. Over time as the binding moves towards saturation, heat release/absorption lessens until finally the only signal remaining is the heat of diluting the syringe sample into buffer. Through the integration of these peaks, a curve can be generated revealing all of the thermodynamic parameters previously mentioned.[38]

Research Aims

To deepen our understanding of the various mechanisms of FVIII inhibition by inhibitory antibodies and how inhibitors compete and cooperate with each other for FVIII binding, the following aims were pursued.

1. Crystallization of isolated C1 domain with human derived anti-C1 inhibitor NB2E9 Fab fragment.
2. Bio-layer interferometry FVIII binding competition assays between anti-A2 domain inhibitors 4A4, 4F4, 1-D4, 4C7, 2-101, and NB11B2.
3. Investigation by isothermal titration calorimetry of cooperativity between inhibitory antibodies G99 and 3E6 in binding the C2 domain of FVIII.

Materials and Methods

Mammalian Cell Growth and Passaging

Hybridoma cell stocks containing ~1 million cells in CryoStor® CS10 from STEMCELL Technologies (CAT#07959) stored in liquid nitrogen were thawed rapidly in a 37 °C water bath and transferred to a sterile 15 mL conical centrifuge tube in a sterile biosafety cabinet (Thermofisher) containing 9 mL Medium E (STEMCELL Technologies, CAT#03805). The cells were pelleted through centrifugation at 1000 rpm at room temperature for 5 minutes and the supernatant was discarded. The cells were then gently resuspended in 5 mL of fresh Medium E and transferred to a T-75 cm^2 flask containing 15-20 mL Medium E. The flasks containing the cells were sealed loosely and placed in a sterile water bath incubator at 37 °C and 5% CO_2. Flasks were observed daily and observations were taken about the color of the media, shape of the cells, and percent confluence. Once the adhered cells reached a percent confluence of 70-80%, cells were washed with 1 mL of Versene (Gibco, CAT#15040066) dissociation agent and the wash was discarded. The cells were then incubated with 5 mL of Versene and placed into the incubator for 5 minutes to loosen the cells from the flask. Following incubation, cells were dissociated from the flask through gentle tapping of the flask. To assess cell viability, 50 µL of the Versene containing the dissociated cells were mixed with 200 µL of Trypan Blue dye (0.4%) (Sigma-Aldrich, CAT#T8154) and a 20 µL aliquot was pipetted into a hemocytometer (INCYTO, DHC-N01). Cell density was determined through counting the number of viable cells in the 1 mm^2 grid and multiplying by the dilution factor. The Versene cell slurry was transferred to a sterile 15 mL conical centrifuge tube for pelleting via centrifugation at RT and 1000 rpm for 5 minutes for either passaging or cell stocks.

Expression of Monoclonal Antibodies in AOF Media

Cells pelleted from the previously mentioned Versene slurry were resuspended in 4 mL AOF media (STEMCELL Technologies, CAT#: 03835). 2 mL of this mixture was added to two separate sterile T-

75 cm^2 flask containing 25 mL of AOF media and placed into the CO_2 incubator for 4-5 days. Once the media was exhausted, and cells were mostly dissociated from the flask indicating cell death, the media was poured into a sterile 50 mL conical centrifuge tube and 10% NaN_3 was added to a final concentration of 0.02%. Cells were pelleted through centrifugation at RT for 5 minutes and the supernatant was sequestered for purification. Patient-derived antibodies NB2E9 and NB11B2 were obtained from Dr. Carmen Coxon at the National Institute of Biological Standards in Potter's Bar, UK.

Protein A Purification of Mouse IgG2ακ Monoclonal Antibodies

Clarified supernatant from hybridoma expression was diluted at least 2x with protein A binding/wash buffer (50 mM HEPES, 150 mM NaCl, pH 8.2) and passed over 1 mL of Protein A resin (ThermoFisher Scientific, CAT#20333). The flow-through was collected and passed back over the column 1-2 times. The column was washed with protein A binding/wash buffer until the flow-through reached an A_{280} of 0. To elute the mAbs from the column, 15 CV of Protein A elution buffer (200 mM glycine, pH 2.85) was passed over the column and collected in a 50 mL conical centrifuge tube containing 0.5 CV of 5 M NaCl and 1.5 CV of 1 M Tris-HCl pH 8.2. Purity of mAbs was assessed via 12.5% SDS-PAGE, and mAbs were dialyzed overnight into TBS (20 mM Tris-HCl, 150 mM NaCl, pH 7.4) for long-term storage at -80 °C.

Protein G Purification of Mouse IgG1 Monoclonal Antibodies

Clarified supernatant from hybridoma expression was diluted at least 2x with protein G binding/wash buffer (20 mM sodium phosphate, 150 mM NaCl, pH 7.2) and passed over 1 mL of Protein G resin (Genscript, CAT#L00209). The flow-through was collected and passed back over the column 1-2 times. The column was washed with protein G binding/wash buffer until the flow-through reached an A_{280} of 0. To elute the mAbs from the column, 15 CV of Protein G elution buffer (100 mM glycine, pH 2.50) was passed over the column and collected in a 50 mL conical centrifuge tube containing 0.5 CV of 5

M NaCl and 1.5 CV of 1 M Tris-HCl pH 8.2. Purity of mAbs was assessed via 12.5% SDS-PAGE, and mAbs were dialyzed overnight into TBS (20 mM Tris-HCl, 150 mM NaCl, pH 7.4) for long-term storage at -80 °C.

Generation of Fab Fragments Through Papain Digestion

Approximately 3 mg of purified mAbs were dialyzed overnight into sample buffer (20 mM sodium phosphate, 10 mM EDTA, 50 mM NaCl, pH 7.2), concentrated down to a volume of 10 mL, and placed into a 15 mL conical centrifuge tube. Cysteine-HCl-H_2O (ThermoFisher Scientific) was added to the mAb solution and the pH was adjusted to 7.0 with ~250 µL of Tris-HCl pH 8.80. A 350 µL slurry of Immobilized Papain Resin (ThermoFisher Scientific, CAT#20341) was equilibrated in freshly prepared digestion buffer (20 mM sodium phosphate, 20mM Cysteine-HCl-H_2O, 10 mM EDTA, pH 7.0) and added to the mAb solution. The volume of the resin/mAb mixture was then adjusted to 13 mL with sample buffer so that the concentration of the added cysteine was 20 mM, and the tube was sealed with parafilm for an overnight water-bath incubation at 37 °C and 150 rpm.

Purification of Fab Fragments with Protein A Resin

Following papain cleavage, the Immobilized Papain Resin was removed from the sample and the pH of the Fab/Fc mixture was adjusted with Tris-HCl pH 8.8 so that it turns the same color as Protein A binding/wash buffer when pipetted onto pH indicator paper. Protein A resin was equilibrated in Protein A binding/wash buffer and added to the mixture for an overnight incubation at 4 °C on a vertical rotating mixer (Benchtop Lab Systems) to remove Fc fragments and undigested mAbs. Fc fragment contamination of Fab fragment samples was assessed first through a binding test to ProA biosensors (Sartorius). If the Fab bound to the ProA biosensor, a second overnight incubation with regenerated Protein A resin was performed to remove trace Fc fragments/undigested mAbs. Final purity was assessed via 12.5% SDS-PAGE and Fab fragments were buffer-exchanged into HBS (20 mM HEPES, 150 mM NaCl, pH 7.4) for long-term storage at -80 °C.

Transformation of hFVIII C1 and C2 Domain-containing Plasmids

Residues spanning the hFVIII C1 and C2 domains were ordered from Genscript as pET32a-TEV(+) plasmids using *BamH1* and *Xho1* restriction sites and an N-terminal His_6-thioredoxin affinity tag. The C1 and C2 constructs were transformed into chemically competent C2039J SHuffle K12 and BL21(DE3) *E. Coli* cells respectively in accordance with New England Biolabs' high efficiency transformation protocol. Transformed Shuffle K12 and BL21 cells were plated on Lysogeny Broth (LB) agar plates containing 1% tryptone (w/v), 1% NaCl (w/v), 0.5% yeast extract (w/v), and 100 µg/mL ampicillin and incubated at 30 °C and 37 °C respectively. Isolated single colonies were harvested from agar plates and allowed to grow in 10 mL of LB at 30 °C for SHuffle K12 cells and 37 °C for BL21 cells. After a 16-18 hour incubation at these temperatures, cell stocks were prepared in 20% glycerol for storage at -80 °C.

Growth and Expression of Human C1 and C2 Wildtype Constructs

Overnight cultures from cell stocks generated from single colonies were grown overnight in 10 mL of LB and transferred to flasks containing 1 L of 2xYT media containing 1.6% tryptone, 1% yeast extract, 0.5% NaCl, and 40 mM $MgCl_2$ and allowed to incubate at 180 rpm until the 600 nm absorbance (OD_{600}) of the cultures reached between 0.6 and 0.8. Flasks were incubated at 30 °C and 37 °C for C1 and C2 constructs respectively. Upon reaching the desired OD_{600} values of 0.6-0.8, flasks were cooled on ice for 1 hour before being placed back into the incubator adjusted to 15 °C. Cells were induced for protein expression through the addition of isopropyl B-D-thiogalactopyranoside (IPTG) to 500 µM and left to express overnight for 18-20 hours.

Cells were pelleted from the cultures through centrifugation at 6371x g for 10 minutes at 4 °C (FIBERLite F10-6x500y rotor, ThermoFisher Scientific, Waltham, MA) and resuspended in 7 mL of cold C1/C2 Lysis buffer (20 mM Tris pH 8.0, 300 mM NaCl, 10 mM imidazole pH 8.0, 0.1% (v/v) Triton X-100, 10% (v/v) glycerol) per 1 gram of pellet in a 250 mL beaker. Following resuspension, 100 mM

phenylmethylsulfonyl fluoride (PMSF) was added to a final concentration of 1mM, followed by 50 mg/mL lysozyme to a final concentration of 1 mg/mL. Cells were enzymatically lysed for 30 minutes at 4 °C on a stir plate set to 100 rpm. Cells were then mechanically lysed using a Branson Sonifier 450 probe at power output 5 and 50% duty cycle for 30 seconds six times with 30 second rest periods in between each cycle. Cell debris was pelleted through centrifugation at 16,500 rpm at 4 °C for 45 minutes (FIBERLite F21- 8x50y rotor, Thermo Fisher Scientific), and the supernatant was decanted into a 250 mL beaker.

Purification of Human C2 Wildtype Construct

Post-lysis high-speed supernatant was loaded onto a 5 mL Hi-trap Ni-NTA column (Cytiva) equilibrated in C1/C2 Lysis buffer connected to a fast protein liquid chromatography (FPLC) device (AKTA Go, Cytiva Life Sciences) at a 3 mL/min flow rate. The column was washed with C2 Wash buffer (20 mM Tris pH 7.4, 300 mM NaCl, 15 mM imidazole pH 7.4) until the UV absorbance at 280 nm (A_{280}) reading on the chromatogram returned to baseline. The flow rate was then switched to 2.5 mL/min and the column was washed with 30 mL ATP Wash buffer (20 mM HEPES pH 7.4, 300 mM KCl, 20 mM $MgCl_2$) made with fresh ATP dissolved to 4.6 mM. This wash was repeated once more and then the column was washed with C2 wash buffer at 3 mL/min until the A_{280} returned to baseline. The column was then washed with 5% C2 Elution buffer (20 mM tris pH 7.4, 300 mM NaCl, 500 mM imidazole pH 7.4) until the A_{280} returned to baseline. A gradient elution from 5-100% Buffer B (C2 Elution buffer) was performed over the course of 100 mL and collected in 4 mL fractions. Fractions were analyzed for purity via 12.5% SDS-PAGE and fractions of interest were pooled and dialyzed overnight at 4 °C into C2 Dialysis buffer (20 mM Tris pH 7.4, 300 mM NaCl) for storage at -80 °C or TEV cleavage during dialysis.

Purification of Human C1 Wildtype Construct

Post-lysis high-speed supernatant was loaded onto a 5 mL Hi-trap Ni-NTA column equilibrated in C1/C2 Lysis buffer connected to a FPLC device set to a flow rate of 3 mL/min. The column was washed with C1 Wash buffer (50 mM Tris pH 8.2, 300 mM NaCl, 10 mM imidazole pH 8.2, 10% (v/v) glycerol) until the A_{280} returned to baseline. The flow rate was then switched to 2.5 mL/min and the column was washed with 30 mL ATP Wash buffer (20 mM HEPES pH 7.4, 300 mM KCl, 20 mM $MgCl_2$) made with fresh ATP dissolved to 4.6 mM. This wash was repeated twice more and then the column was washed with C1 wash buffer 3 mL/min until the A_{280} returned to baseline. The column was then washed with 5% C1 Elution buffer (50 mM Tris pH 8.2, 300 mM NaCl, 500 mM imidazole pH 8.2, 10% (v/v) glycerol) until the A_{280} returned to baseline. A gradient elution from 5-100% Buffer B (C1 Elution buffer) was performed over the course of 100 mL and collected in 4 mL fractions. Fractions were analyzed for purity via 12.5% SDS-PAGE and fractions of interest were pooled and dialyzed overnight at 4 °C into C1 Dialysis buffer (20 mM tris pH 8.2, 300 mM NaCl, 10% (v/v) glycerol) for storage at -80 °C or TEV cleavage during dialysis.

TEV Cleavage of C2 Wildtype Construct

Purified C2 wildtype was cleaved overnight at 4 °C during dialysis into C2 dialysis buffer by the addition of 1 mg of purified TEV protease for every 10 mg of C2 present. The following day, the cleavage mixture was loaded onto a 5 mL Hi-trap Ni-NTA column equilibrated in C2 wash buffer connected to an FPLC. Cleaved C2 weakly bound to the column was eluted through washing with 3% C2 Elution buffer and 97% C2 wash buffer until the A_{280} returned to baseline. Eluent was then concentrated to 5 mL for and loaded onto a 120 mL S75 column (GE Healthcare) equilibrated in 20 mM Tris pH 7.4 and 100 mM NaCl for buffer exchanging via size-exclusion chromatography (SEC). Peaks of interest were collected into a 50 mL conical centrifuge tube and purity was assessed via 12.5% SDS-PAGE.

TEV Cleavage of C1 Wildtype Construct

Purified C1 wildtype from FPLC immobilized metal affinity chromatography (IMAC) purification was cleaved overnight at 4 °C during dialysis into C1 dialysis buffer by the addition of 1 mg of purified TEV protease for every 10 mg of C1 present. The following day, the cleavage mixture was loaded onto a 5 mL Hi-trap Ni-NTA column equilibrated in C1 wash buffer connected to an FPLC. Cleaved C1 weakly bound to the column was eluted by washing with 6% C1 Elution buffer and 94% C1 wash buffer until the A_{280} returned to baseline. Purity of eluent was assessed via 12.5% SDS-PAGE. If molecular chaperones were present in the sample following SDS-PAGE analysis, C1 was dialyzed into C1 High-salt dialysis buffer (20 mM Tris pH 8.2, 500 mM NaCl, 10% glycerol) to release the chaperones from C1. The C1-chaperone mixture was then passed back over the Ni-NTA FPLC column in an identical manner to the previous post-cleavage step. Purity was again assessed via 12.5% SDS-PAGE. Once sufficient purity was reached, the eluent was concentrated to 5 mL and loaded onto a 120 mL S75 column (GE Healthcare) equilibrated in 20 mM Tris pH 7.4 and 100 mM NaCl for buffer-exchanging via SEC. Peaks were collected and stored at -80 °C.

Formation of FVIII:Antibody Complexes

For the complexes used in the anti-A2 domain mAb BLI competition assays, 200 nM stock solutions of Et3i, 4A4, NB11B2, 4F4, 1D4, and 4C7 Fab fragments were first prepared through dilution with HBS. Complexes were formed at 200 nM by combining 25 µL of the 200 nM Et3i stock with 25 µL of each 200 nM anti-A2 domain Fab stock. The complexes were placed on ice for 20 minutes and mixed intermittently.

To prepare the C1-NB2E9 Fab complex for protein crystallography, TEV cleaved C1 WT was combined in a 1:1.2 stoichiometric ratio with the NB2E9 Fab fragment and allowed to sit on ice for 20 minutes with intermittent mixing. The complex was buffer exchanged into 20 mM HEPES pH 7.4 and 200

mM NaCl in a 4 mL 30 kDa MWCO Amicon spin concentrator. The complex was concentrated to 1.75 mg/mL in the same concentrator and stored in 25 µL aliquots at -80 °C.

To prepare the complex of the cleaved C2 WT and G99 Fab fragment for ITC, C2 WT and the G99 Fab fragment were combined in a 1.4:1 stoichiometric ratio of C2 to G99 Fab. After sitting on ice for 20 minutes, the complex was concentrated to 500 µL in a 4 mL 10 kDa MWCO Amicon spin concentrator and loaded onto a 24 mL S75 column (GE Healthcare) for removal of excess C2 WT. Once the complex was homogenized through SEC, it was concentrated to 3 µM in the same spin concentrator and stored at -80 °C in 500 µL aliquots.

Bio-layer Interferometry (BLI) Antibody Competition Assays

To determine how anti-A2 domain mAbs compete with each other to bind the A2 domain of FVIII, competition assays at room temperature were performed using a BLitz (ForteBio) instrument alongside BLITz Pro software (ForteBio) for data analysis. To establish a baseline, ProA biosensors (Sartorius) stored in HBS were submerged in 200 µL HBS for 30 seconds. 4 µL of each anti-A2 domain mAb at 200 nM was then loaded to the biosensor for 120 seconds. After a 30 second wash in 200 µL HBS, 4 µL of a 200 nM Et3i-competing Fab complex was associated to measure whether or not the mAb immobilized on the tip is capable of binding Et3i when a competing Fab is present. Finally, a 120 second dissociation step was carried out to check whether Et3i stays bound in the presence of the competing Fab-Et3i complex. Each experiment was carried out in triplicate.

If no binding was observed, the inverse experiment was performed to validate the results. This means that the competing Fab was loaded onto the tip as a mAb, and the Et3i-Fab complex of the mAb formerly on the tip was associated. If binding was observed in triplicate between the mAb and the Et3i-Fab complex, the inverse experiment was not performed. Controls in which each of the five anti-A2

domain mAbs are loaded to the tip and bound to Et3i alone were performed, as well as controls showing how strongly the Fab used to make each complex binds to the tip.

Regeneration of ProA BLI Biosensors

To ensure that no false-positives were recorded when performing BLI competition assays, a new method for regenerating BLI biosensors was employed. Immediately after use, tips were soaked for 5 seconds in Biosensor Regeneration Buffer (20 mM glycine pH 1.5) and then in HBS for 5 seconds. This process was repeated 2-4 more times and the tips were then returned to their container, remaining hydrated in fresh HBS. Tips were reused up to 5 times before being deemed unfit for binding assays.

Isothermal Titration Calorimetry Antibody Binding Experiments

ITC binding experiments involving the 3E6/G99 mAbs against C2 WT as well as the 3E6 mAb against the C2-G99 Fab complex were performed in duplicate on a MicroCal VP-ITC. Each experiment was conducted in high-feedback mode at 35 °C with a stirring speed of 351 rpm, a reference power of 20 µCal/second, and an initial delay of 60 seconds. All sample and buffer solutions used for ITC were degassed for 15 minutes prior to usage in a Malvern MicroCal ThermoVac Sample Degassing Thermostat. All samples were buffer-exchanged into ITC buffer (20 mM Tris pH 7.4, 100 mM NaCl) prior to usage through overnight dialysis or SEC. They were then diluted with this buffer to the concentrations listed below. In the syringe, 300 µL of either 3E6 or G99 mAb at 6.25 µM was loaded from a 400 µL sample. In the cell, 1.8 mL of either C2 WT or the C2-G99 Fab complex was loaded from a 2.25 mL sample at 1.25 µM. Into the reference cell, 1.8 mL of degassed ITC buffer was loaded. A total of 19 injections were made during the experiments, with the first injection being a 2 µL injection over the course of 4 seconds. The following 18 injections were 15 µL injections with a duration of 30 seconds per injection and a spacing of 210 seconds between injections. Heat of dilution experiments were performed for both the 3E6 and G99 mAbs in which each mAb was loaded into the syringe at 6.25 µM

and injected into a cell containing just ITC buffer using the same experimental parameters mentioned above. A linear regression was performed on this data and it was then subtracted from the initial dataset involving the same mAb in the syringe to yield the final thermogram. Values of thermodynamic constants, reaction stoichiometry, and K_D were calculated by the MicroCal Analysis software (Malvern) upon applying a nonlinear one set of sites curve fit to the data.

Results and Discussion

Expression and Purification of the Human C1 Domain

Successful expression and purification of the human C1 domain of FVIII was achieved using adapted versions of procedures developed by previous Spiegel lab members. In a manner no different from prior expressions of C1, SHuffle K12 *E. Coli* cells proved to express C1 in the greatest abundance. Purification however, was altered in a variety of ways as pure protein could not be produced using past methods. To start, rather than using TALON cobalt resin packed into a gravity flow column to bind the protein for purification, a 5 mL Ni-NTA column connected to an FPLC was used to better visualize contaminants coming off the column. As the isolated C1 domain contains a great amount of surface-exposed hydrophobic residues and suffers from instability because of this, wash and elution buffers for this purification were adjusted from pH 7.4 to 8.2. This was done in an effort to increase the solubility of the protein by moving the pH further from its isoelectric point (pI) of 7.3 to increase its net charge in solution. Conveniently, this pH lies just in between the pIs of cleaved and tagged C1. Since cleaved C1 has a pI of 9.9, this pH is suitable for performing a TEV cleavage. The concentration of ATP in the ATP wash buffer was lowered from 10 mM to 4.6 mM as significant amounts of protein appeared to elute from the column when using the higher concentration of ATP as shown by post-IMAC SDS-PAGE analysis (Figure 7).

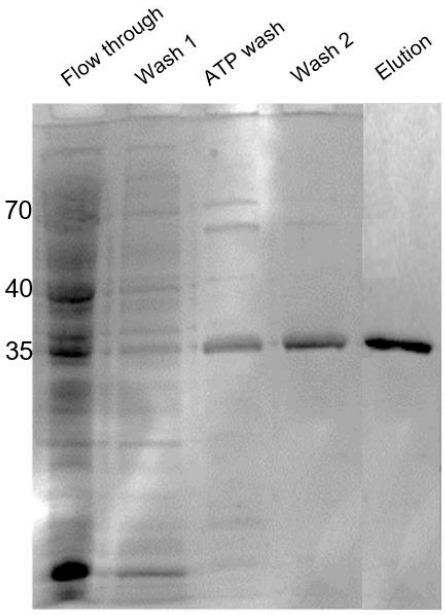

Figure 7. Purification of C1 WT via Ni-NTA IMAC.

TEV Cleavage of C1 WT

The N-terminal thioredoxin fusion tag and hexahistidine tags were removed from the C1 WT construct in order to provide an accurate representation of the protein in its native state for structural determination via X-ray crystallography. Initially, the purified protein was incubated with TEV protease during overnight dialysis into 20 mM MES pH 6.0, 300 mM NaCl, and 10% (v/v) glycerol. But upon analysis of the pIs of tagged and cleaved C1, it was found that this dialysis buffer placed the nascent cleaved product into an environment in which it was nearly 4 pH units away from its PI, and therefore incredibly unstable. Additionally, the elution buffer at pH 7.4 that the tagged C1 was collected in placed tagged C1 into a buffer 0.1 pH units from its pI, decreasing its net charge and stability. This was reflected visually in the cleavage mixture as significant amount of precipitated protein in dialysis was usually visible the following day. Upon changing the dialysis and purification buffers to Tris pH 8.2, this issue was for the most part resolved. Precipitation of C1 still occurred during dialysis during this method, but to a lesser extent. This is likely due to C1's general lack of stability as an isolated construct.

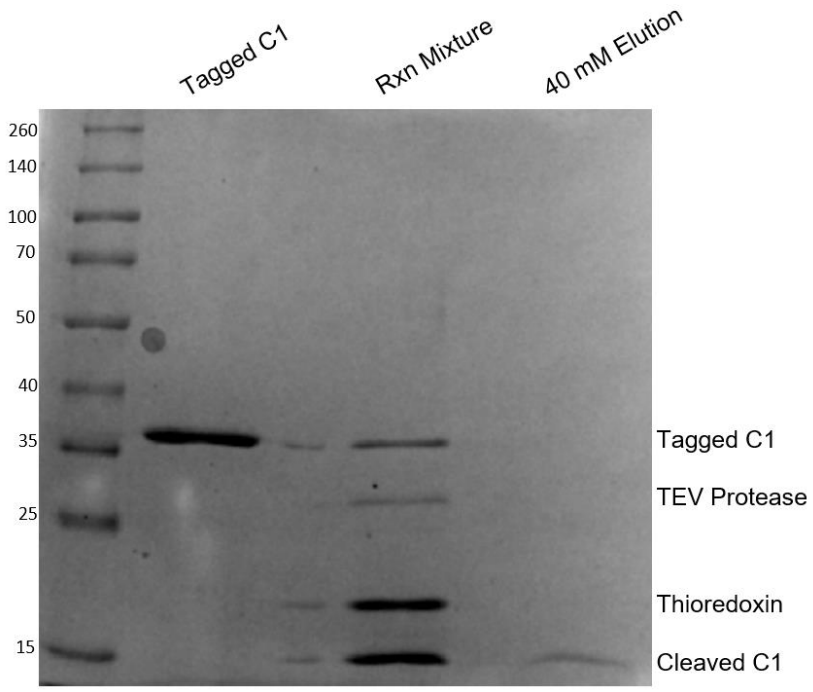

Figure 8. TEV cleavage and purification of cleaved C1 WT.

To separate the cleaved product from the cleavage mixture, the mixture was loaded onto a Ni-NTA FPLC column. In a typical purification of a TEV cleavage mixture, remaining tagged protein, His-tagged TEV protease, and the thioredoxin tag bind to the column, while the cleaved protein does not and is collected in the flow-through. But following examination of the flow-through via SDS-PAGE, it was discovered that this was not the case as no protein of any sort was present. This implies that the cleaved protein was binding to the column. To mitigate this, a gradient elution was performed on the column in order to find the lowest concentration of imidazole required to elute the cleaved protein from the column, which should bind more weakly than the other species present. This concentration ended up being 40 mM imidazole. When eluting the column at this concentration, pure cleaved C1 was obtained (Figure 8). Occasionally, the cleaved C1 sample contained a band at 70 kDa identified to be *E. coli* heat-shock protein DnaK (Hsp70). This was solved by re-dialyzing overnight into the same dialysis buffer containing 500 mM NaCl rather than 300 mM and repeating the previously mentioned purification process.

Crystallization of the C1:NB2E9 Complex

To deepen our understanding of how inhibitory antibodies decrease or abolish FVIII activity through binding to the C1 domain, crystallographic trials were performed on the complex of C1 WT with inhibitor NB2E9. The conditions yielding the most promising crystals was 100 mM MES pH 6.5, 300 mM $MgCl_2$, 19-19.5% PEG 4000, and 100 µL Al's Oil. Promising crystals were also observed in the condition 100 mM sodium acetate pH 5.0, 60-80 mM ammonium thiocyanate, and 17.5% PEG 8000. Images of these crystals are shown in Figure 9A and B.

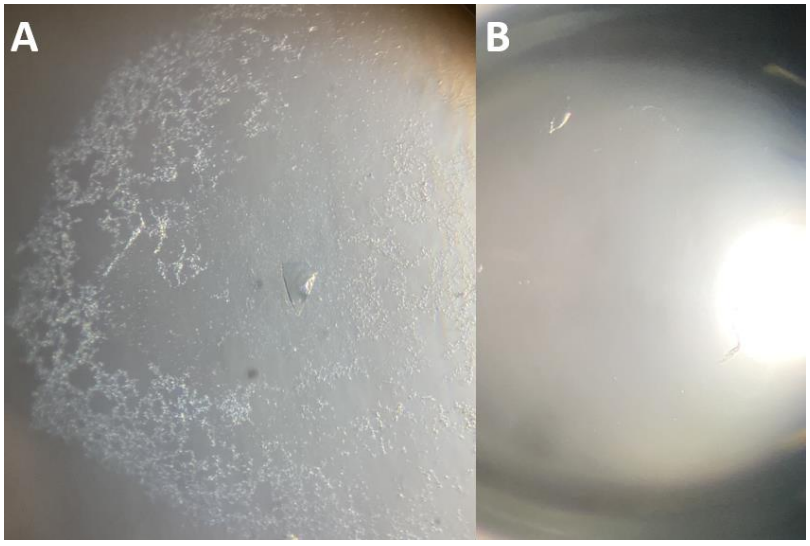

Figure 9. A) C1:NB2E9 crystal formed using a 1:1 ratio of protein stock to mother liquor in 100 mM MES pH 6.5, 300 mM $MgCl_2$, 19% PEG 4000, with 100 µL Al's Oil applied to the top of the well solution. B)) C1:NB2E9 crystal formed using a 1:1 ratio of protein stock to mother liquor in 100 mM Sodium Acetate pH 5.0, 60 mM Ammonium thiocyanate, and 17.5% PEG 8000.

Despite the successful formation of protein crystals for this complex, no diffraction was observed during data collection on the SIBYLS beamline 12.3.1 at the Advanced Light Source (ALS) Berkeley Center for Structural Biology (BCSB). While these conditions did show promise, further analysis was discontinued as fellow Spiegel lab member Dr. Kenny Childers gathered high-quality (Cryo-EM) data on this antibody in complex with BDD-FVIII construct Et3i. A structure of full-length BDD-FVIII in complex with NB2E9 is the ideal presentation of NB2E9's interactions with FVIII, and a structure of isolated C1

with NB2E9 only possesses the advantage of a potential higher resolution at the epitope. As discussed in the next section however, the global resolution for the Et3i:NB2E9 structure is more than sufficient to reveal the depth of NB2E9's inhibitory mechanism when bound to FVIII.

Cryo-EM Structure of Et3i in Complex with NB2E9

Although crystallography with the isolated C1 domain in complex with the NB2E9 Fab fragment was unsuccessful, K. Childers found success in the structural determination of Et3i in complex with NB2E9 to an average global resolution of 3.67 Å through Cryo-EM (Figure 10). Although this specific method of structural determination was not involved in the aims of this work, the Fab fragment used to form the Et3i:NB2E9 complex was produced and purified by the author of this thesis.

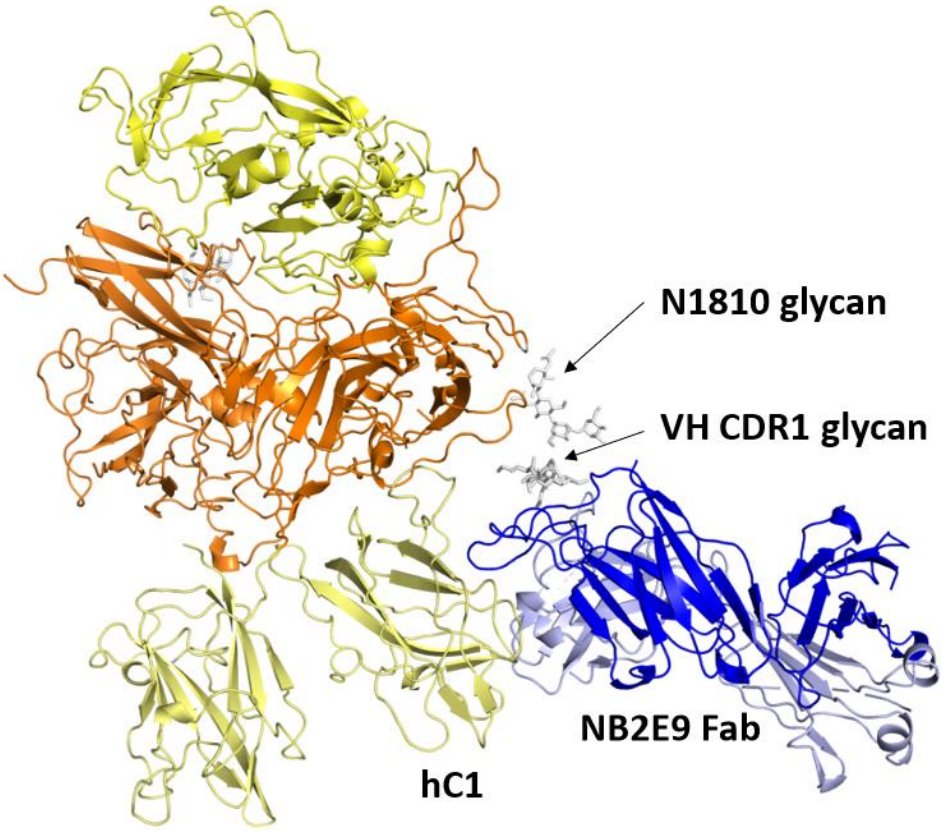

Figure 10. Cryo-EM structure of Et3i bound to inhibitor Fab fragment NB2E9 illustrating glycosylation on FVIII residue N1810 and NB2E9 VH CDR1 residues 47-49 (K. Childers, unpublished data).

An advantage of Cryo-EM when compared to X-ray crystallography is that Cryo-EM resolution varies throughout the structure, when the latter possesses a consistent resolution throughout each part of the structure. This can be a disadvantage as well, as some more flexible regions such as the C2 domain may show resolutions far worse than their crystal structure counterparts. Despite this, every region in this structure falls within the acceptable resolution range for crystallography, with many regions such as the epitope having much higher resolution than other FVIII crystal structures. FVIII is a heavily glycosylated protein, and this has allowed some of its glycans to finally be modeled into its structure, such as the glycan located at FVIII residue N1810, which appears to be interacting with NB2E9 (Figure 10).

This structure overlaps well with present literature relating to NB2E9/LE2E9's interactions with FVIII. Previous mutational analyses of FVIII identified E2066 as a significant binding residue for LE2E9, as its binding to FVIII was completely abolished upon substitution of this residue.[39] In the Cryo-EM structure of this Et3i:NB2E9, this residue serves as a crucial point of contact between NB2E9 and Et3i. This structure also visualizes the Asn-linked glycan found on residues 47-49 in the CDR1 region of the NB2E9 heavy chain (Figure 10).[31] While the removal of this glycan has been previously shown to significantly decrease NB2E9's inhibitory capabilities, no apparent interactions between this glycan and FVIII are visible in this structure. However, a structural overlay of the cryo-EM structure of vWF bound to FVIII with this structure suggests that this glycan is responsible for the blocking of the D' region of vWF. This explains previous observations noting the interference with FVIII:vWF interactions by LE2E9.

This antibody behaves similarly to 2A9, an antibody produced by hemophiliac mice when injected with recombinant FVIII. Both antibodies inhibit FVIII binding through binding interference with vWF.[29] When comparing the crystal structure of Et3i:2A9 to the Cryo-EM structure of Et3i:NB2E9, a large overlap between the two epitopes can be seen. Although a structure of a human antibody bound to FVIII is ideal, the solving of this crystal structure highlights the similarities between mammalian immune

responses to injected FVIII and validates the merit of antibody inhibition studies on species other than humans.

Production of Monoclonal Antibodies from Mouse Hybridoma Cells

In hopes of determining how inhibitory antibodies compete with each other for binding of the FVIII A2 domain, five unique monoclonal antibodies were grown from cell stocks produced by the Lollar lab at Emory University. These antibodies consisted of 4A4, 4F4, 1D4, 4C7, and 2-101. To begin the process typically used in the Spiegel lab, cells are thawed and placed for 7-10 days into Medium E, a nutrient-rich growth medium designed to promote growth of healthy cells. As hybridomas are a stable cell line, they constantly produce antibodies when in a viable state. However, when looking to extract pure antibodies from a Medium E culture, great difficulty is encountered due to the abundance of other proteins found in the media. To combat this, the cells are allowed to grow in Medium E until they reach 50% confluence and are then transferred to the serum-free AOF media where viable cells can produce antibodies in a relatively simpler environment. The cells are then allowed to express antibodies for up to 10 days or until the media is visibly nutrient-deficient, indicated by its color (Figure 11). Finally, the cells are killed with NaN_3 and the media is sequestered for purification.

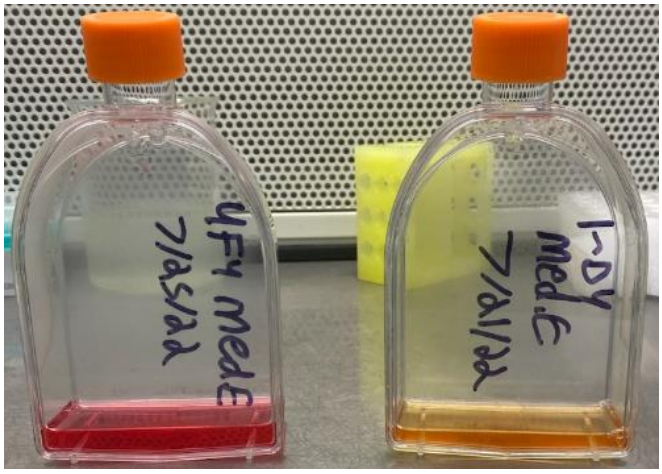

Figure 11. Medium E cultures containing fresh media and newly passaged cells (left) and exhausted media with cells ready to be passaged (right).

Using methods previously proven successful in the Spiegel lab, yields were significantly lower upon harvest. This was eventually attributed to the diminishing ability of hybridoma cells to produce a given protein the more times they undergo passaging. This problem stemmed from available cell stocks having been prepared from cells passaged several times. Sufficiently healthy cells were obtained through having the cells undergo 3 passage cycles each occurring at ~60% confluence in Medium E prior to expression in AOF. For each passage, ~5% of the cells were passaged into a new Medium E flask and allowed to reach 60% confluence once more. Cell populations from the third passage contain little to no weakened cells damaged by the freeze-thaw cycle that would have been present had they been passaged directly into AOF. Low confluence was chosen for these passages as hybridomas tend to be less healthy in a high-confluence setting, where cells press up against each other and potentially burst. After the third passage, cells were grown to 70-90% confluence depending on apparent cell viability and passaged into two AOF flasks for expression, where they lived for 4-5 days. Media that was used for longer than this period typically yielded vastly lower amounts of antibodies post-purification.

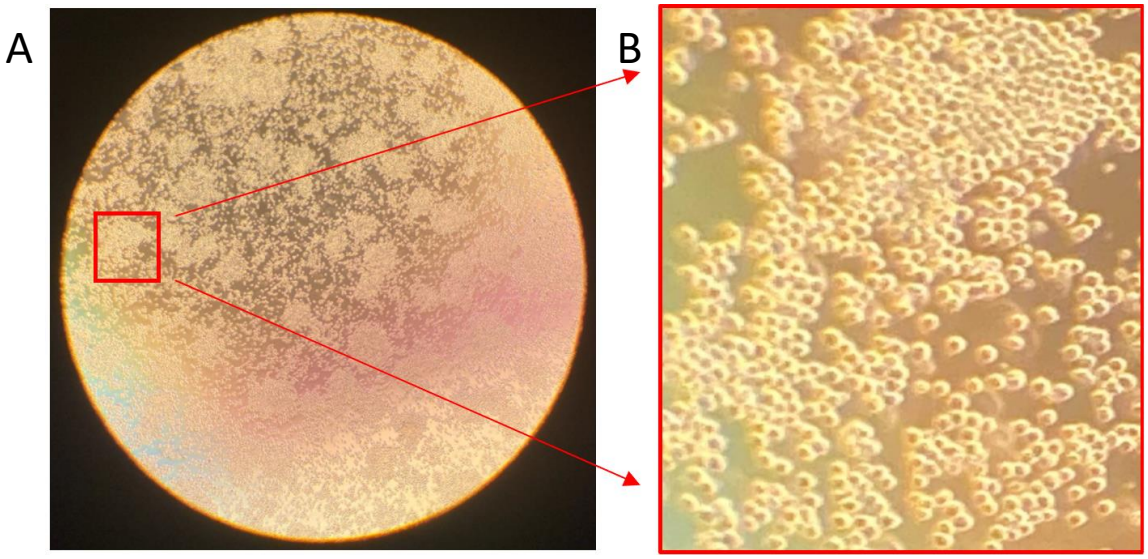

Figure 12. A) Growth-phase hybridoma cells observed under a light microscope. B) Zoomed-in growth-phase hybridoma cells at ~90% confluence.

Protein A and G Purification of Monoclonal Antibodies

Initially, low-yield purifications of 4A4, 4F4, 1D4, 4C7, and 2-101 were performed starting with the 2x dilution of the AOF supernatant with Protein A binding/wash buffer being passed over a Protein A column once. The column was then washed with 5 CV of binding/wash buffer and subsequently eluted with 15 mL of Protein A elution buffer. While this method produced modest amounts of mAbs, their purity was rarely sufficient. This was due to the presence of a ~70 kDa band consistently appearing in the elution lane in an SDS-PAGE gel (Figure 13A). This contaminant was proposed to be bovine serum albumin (BSA), a major component of fetal calf serum, which is found in Medium E. BSA is commonly used to stabilize monoclonal antibodies in storage, allowing antibodies to more easily retain their original conformation in solution.[40]

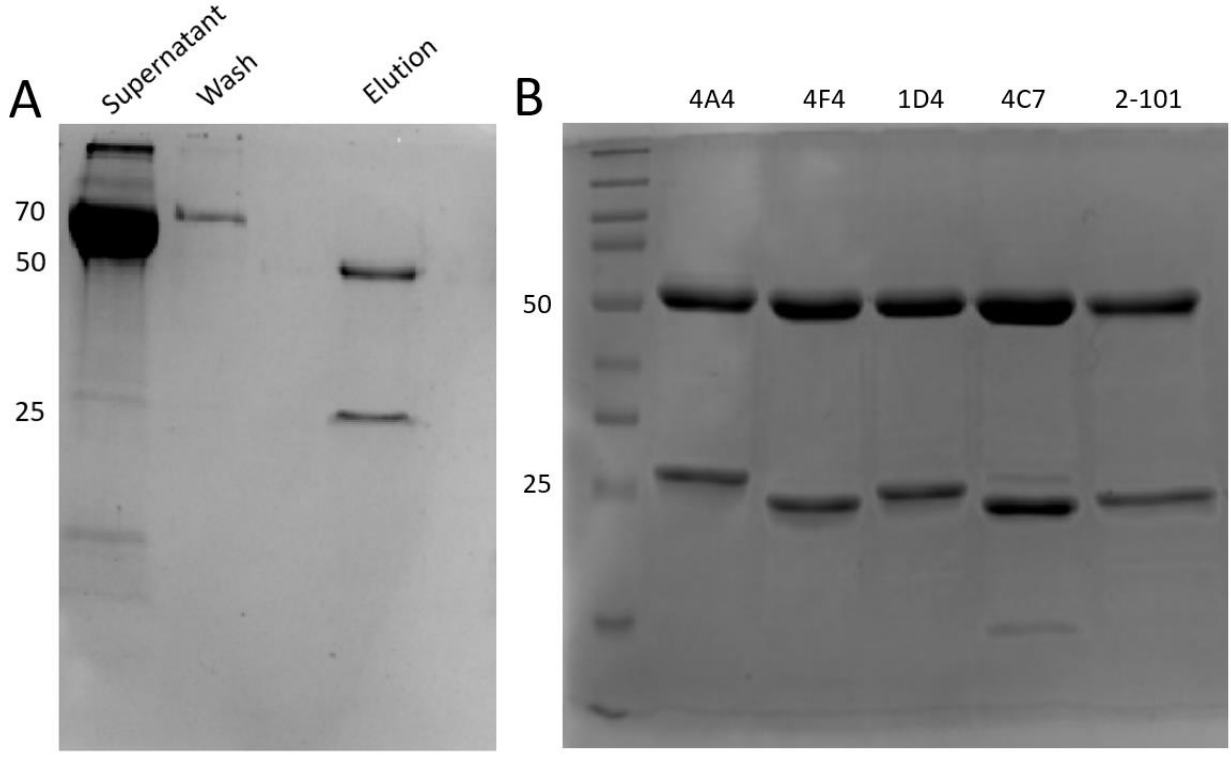

Figure 13. A) Protein A purification of mAb 4A4 from hybridoma supernatant. Removal of contaminating BSA shown in wash lane at ~70 kDa, IgG heavy and light chains shown at 50 and 25 kDa in elution. B) SDS-PAGE gel image depicting anti-A2 domain murine mAbs 4A4, 4F4, 1D4, 4C7, and 2-101 purified via protein A or G chromatography from hybridoma supernatants.

Yields were increased and contaminants were prevented through two different solutions. In an effort to extract larger quantities of mAbs from the hybridoma supernatant, the diluted supernatant was passed over the column a total of 3 times before beginning the washing step. BSA was completely removed from the column through washing to baseline A_{280} rather than with a specific amount of buffer each time (Figure 13A). For a 1 mL Protein A column, this process took 100-150 mL of binding/wash buffer.

Among the five anti-A2 domain mAbs, 2-101 in particular had much lower yields initially from Protein A purification. Upon examining the isotypes of each mAb, it was noted that all mAbs except for 2-101 were mouse IgG2ακ. IgG2ακ mAbs bind strongly to Protein A, explaining the successful purifications of each one. 2-101 however, is of the subclass mouse IgG1, which does not bind as strongly as IgG2ακ mAbs to Protein A. Instead, it binds much tighter to Protein G. As a result, Protein G resin was used to purify 2-101, which greatly increased yields. After the optimization of protein A and G purification methods, sufficient amounts of each antibody were successfully purified (Figure 13B).

Generation of Fab Fragments Through Papain Digestion

Prior to this work, mAbs were partially buffer-exchanged into papain digestion buffer in a spin concentrator and placed into a shaking water bath overnight to be cleaved by Immobilized Papain resin overnight. This resulted in a large amount of protein precipitation visible in the cleavage mixture the following morning. For an ideal papain cleavage, the reaction mixture must contain 20 mM cysteine, and occur at pH 7.0. Due to the nature of this method, this was not the case. When cysteine-HCl-H_2O is dissolved in solution, it can drop the pH of the sample buffer from pH 7 to pH 4-5. This means that with the original method, the cleavage was taking place in an acidic environment, unsuitable for mAb solubility at high temperatures. The cysteine concentration was also likely less than 20 mM, which could have decreased the activity of the papain enzyme.

Successful cleavage in which no precipitates were formed was achieved through a variety of changes to this protocol. Antibodies were dialyzed overnight into Papain sample buffer, concentrated down to a small volume, and cysteine was added as a solid to achieve a final concentration of 20 mM directly to the dialyzed mAb. Upon this addition, the pH was readjusted to 7.0 through the addition of a suitable amount of Tris-HCl pH 8.80. Multiple overnight incubations with Protein A resin were carried out to remove essentially all uncleaved mAb and cleaved Fc fragments from the mixture to produce a very pure Fab sample.

Pure 2-101 Fab was never successfully purified using this method. This is due to the fact that Protein A resin is used to remove Fc and mAb from the cleavage mixture. As mentioned previously, this cannot work since 2-101 binds weakly to Protein A. This process was attempted with Protein G resin as well but only the uncleaved mAb appeared to be removed completely. Protein G binds to Fab fragments as well, which ended up causing a significant removal of Fab fragments from the mixture. It is likely that using ion-exchange chromatography to isolate the Fab could prove successful, but this was not attempted.

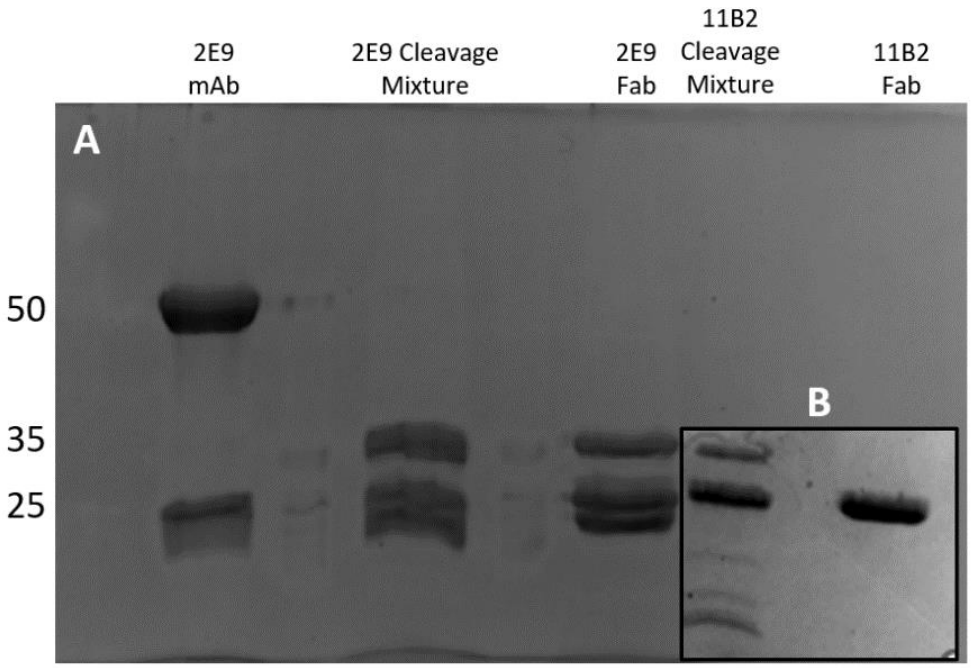

Figure 14. Fab fragment generation through papain digestion. A) SDS-PAGE gel image depicting the cleavage of mAb NB2E9 showing two bands at ~25 kDa, and one band at ~35 kDa. B) SDS-PAGE gel image depicting the cleavage of mAb NB11B2 to produce a Fab fragment appearing as two overlapping bands at ~25 kDa.

Interestingly, the Fab fragment of NB2E9 appeared on an SDS-PAGE gel as three bands, rather than the characteristic two (Figure 14B). These consisted of one band at roughly 35 kDa, and two bands close to 25 kDa (Figure 14A). With the majority of the Fabs in this study, the Fab fragment appeared solely as the two bands near 25 kDa. The only involved species that ever appeared at 35 kDa was the Fc region. This species was confirmed to not bind to protein A resin, as multiple overnight protein A incubations did not reduce the intensity of this band. The sample also failed to bind to ProA BLI tips, which rules out the possibility of it being the Fc region. NB2E9 however, is unique to most other mAbs in that it is glycosylated. Specifically, just one of its two heavy chains per Fab fragment contains this glycan.[39] Glycosylation of a heavy chain region would indeed slow the migration of the protein on a reducing polyacrylamide gel, so it is possible that the 35 kDa band can be identified as a single glycosylated heavy chain molecule. This however was never confirmed. Mass spectrometry analysis of this Fab could be used in the future to confirm that this species is part of the Fab fragment.

Anti-A2 Domain Inhibitor Competition Assays

To better understand how inhibitors compete with each other to bind the A2 domain of FVIII, a set of BLI competition assays was designed and carried out. To assess epitope overlap, mAbs were bound to the ProA biosensor and once a baseline was established, a complex of Et3i and a competing Fab was associated to the tip. If the complex bound to the mAb on the tip, the two antibodies likely do not compete with each other for FVIII binding. If the complex failed to bind, it was decided that the two mAb epitopes overlap. A positive control was run for each mAb on the tip binding to Et3i not in complex with another inhibitor. In some cases, the Fab on its own bound to the tip, indicating slight amounts of uncleaved mAb or Fc region. To determine how much of the binding of the complex to the tip-bound mAb could be attributed to the Fab binding to the tip, each Fab used to make the complex was loaded to the tip. The results for these assays are pictured below in Figure 15.

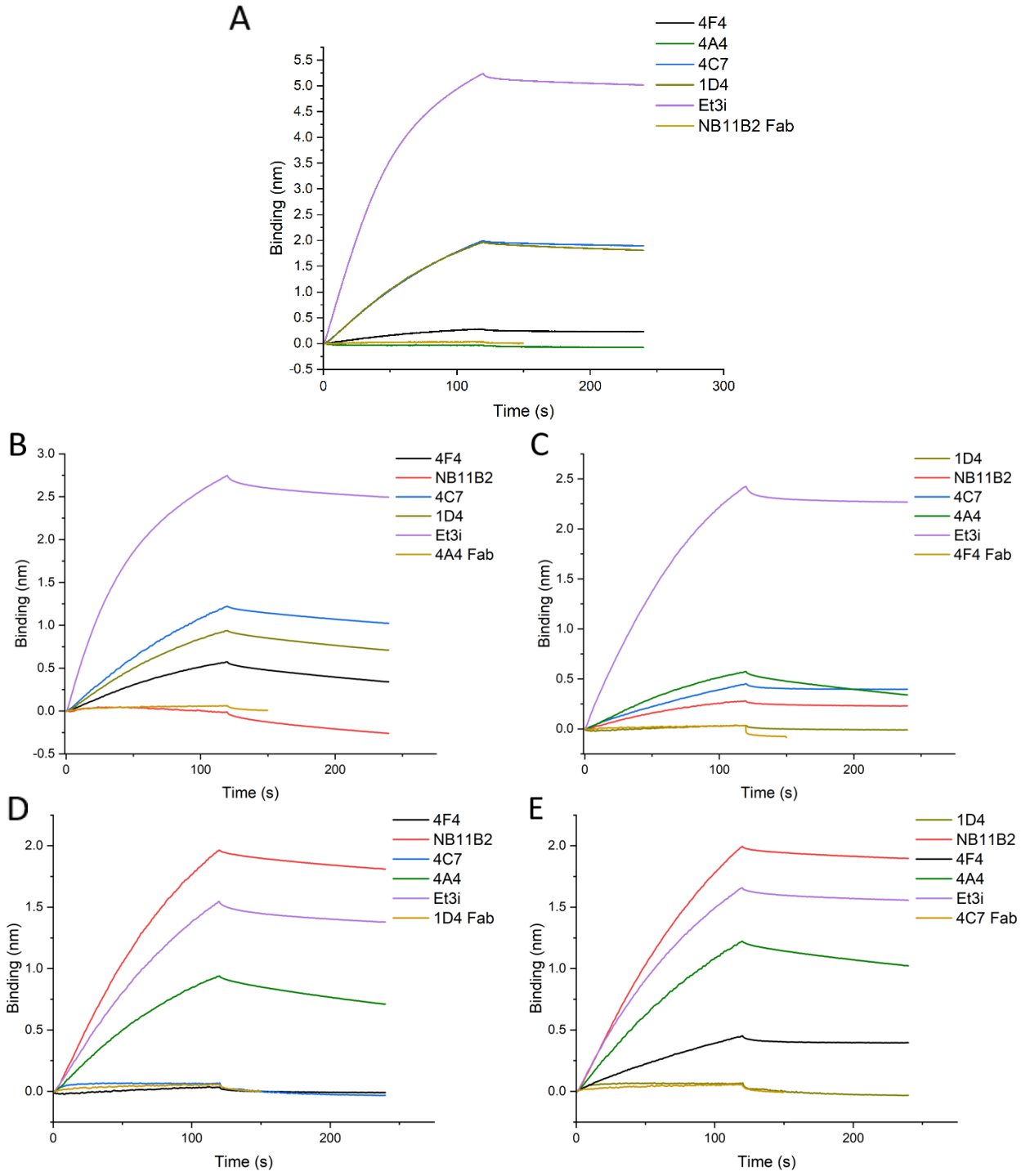

Figure 15. Association-dissociation curves for Et3i in complex with anti-A2 Fabs 4F4, 4A4, 4C7, 1D4, and NB11B2 binding to anti-A2 domain mAbs 4F4, 4A4, 4C7, 1D4, and NB11B2. Et3i Fab complexes were allowed to associate to the tip-bound NB11B2 for 120 seconds, and dissociation was measured over a span of 120 seconds. Fab tip association was measured for 120 seconds, and dissociation was measured for 30 seconds. A) NB11B2 mAb against Et3i-Fab complexes. B) 4A4 mAb against Et3i-Fab complexes. C) 4F4 mAb against Et3i-Fab complexes. D) 1D4 mAb against Et3i-Fab complexes. E) 4C7 mAb against Et3i-Fab complexes.

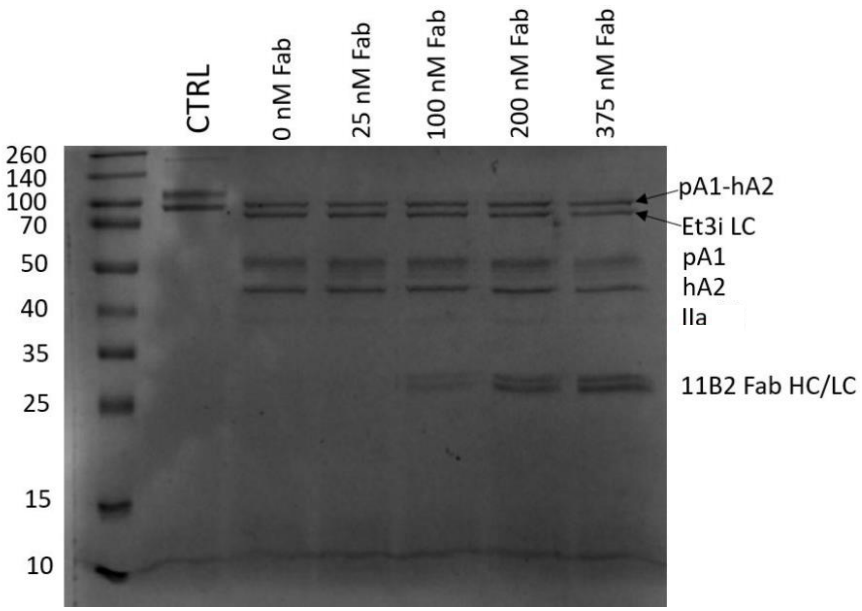

Figure 16. SDS-PAGE gel depicting the one-hour activation of Et3i (150 nM) by thrombin/Factor IIa (30 nM) in the presence of the NB11B2 Fab fragment (0-375 nM). CTRL = Et3i not exposed to thrombin/NB11B2 Fab.

Competition between NB11B2 and other A2 domain inhibitors was largely unstudied prior to this work. Looking to Figure 15A, it appears to completely block FVIII binding of group A inhibitor 4A4. Group A inhibitors bind to the FVIII A2 domain with epitopes ranging from Arg484 to Ile508. The cryo-EM structure of FVIII bound to NB11B2 reveals the epitope to be two points of FVIII contact at residues 491-498 and 501-509 (K. Childers, unpublished data). This data aligns well with the proposed epitope range of residues 379-546 listed in the U.S. patent filed by Jacquemin et al. in 2010 when this inhibitor was initially isolated from a patient and termed BOIIB2.[41] Because this inhibitor significantly impedes the binding of group B mAb 4F4 (Figure 15A), this antibody can perhaps be classified as group AB as its epitope lies on the upper bound of group A mAbs. Since NB11B2 completely overlaps with 4A4, it is likely that this antibody interferes with the formation of the intrinsic tenase complex in some way. Looking to the cryo-EM structure of this inhibitor bound to FVIII however, NB11B2 does not appear to disrupt FIXa binding to FVIII. This observation was made by comparing this structure to a previously proposed SAXS model of the intrinsic tenase complex bound to a lipid nanodisc. Additionally, the possibility of NB11B2's interference with FVIII thrombin activation is seemingly ruled out by the results

shown in Figure 16. Here, Et3i was incubated with thrombin and successfully activated despite the presence of the NB11B2 Fab fragment.

Group A inhibitor 4A4 interferes with the binding of group B inhibitor 4F4, but does not completely block it (Figure 15B). The observations that 4A4 does not compete with 4F4, 1D4, or 4C7 are consistent with the sandwich ELISA A2 domain inhibitor competition assay results performed by Markovitz et al.[26] 4F4 solely blocks binding of group E mAb 1D4, and seems to decrease relative binding of all other tested inhibitors without completely blocking them. This could perhaps be due to steric effects. The overlap between 1D4 and 4F4 is not supported by the competition assays performed by Markovitz et al. The results discussed by this group in fact do not show 4F4 competing with any group E mAbs for FVIII binding.[26] In their findings however, group E inhibitors 4C7 and 2G10 overlap with group B inhibitors G139, B94, G6, and G4.[26] It is unclear which observation describes the true nature of 4F4's competition with other inhibitors, but their findings at least show that overlap between group B and E inhibitors does indeed occur. Aside from this, 4F4's lack of overlap with 4C7 and 4A4 is supported by the findings of Markovitz et al.

1D4 possesses an overlapping epitope with 4C7 and 1D4, and does not compete for FVIII binding with 4A4 and NB11B2. All of these observations are supported by the work of Markovitz et al.[26] The other tested group E mAb, 4C7, competes only with 1D4 as reflected in Markovitz's competition assay results. The last A2 domain inhibitor grown in the Spiegel lab, 2-101, has still not been classified into a group following this work. Competition between this inhibitor and other anti-A2 domain antibodies could not be assessed through BLI due to the design of this assay. This assay used ProA biosensors, and as shown by the difficulty of protein A resin purification of 2-101, 2-101 failed to bind strongly to the biosensors and completely dissociated from the tip following the post-loading baseline step. A FVIII:2-101 Fab complex could also not be formed due to the nature of the current method for isolating Fab fragments with protein A resin. This problem could perhaps be addressed through a slightly different BLI

competition assay in which a FVIII:2-101 mAb complex could instead be associated to a competing antibody on the biosensor. To discern the amount of observed association coming from the mAb complex weakly binding to the tip, a baseline in which the complex loads and dissociates from the tip could be established and compared to the competition assay data.

It is worth noting that initially, many false positives were observed in which the Et3i-Fab complex bound to the tip on its own, not in the presence of an anti-FVIII mAb. The tips being used at this point had been regenerated several times, and likely had antibodies irreversibly bound to them. Upon researching this phenomenon, it was determined that the present method for regenerating tips was damaging the tips. Previously, tips were allowed to sit in HBS after a run with the mAb and Et3i complex still bound to the tip until no more tips were available. The tips were then incubated in 200 mM glycine pH 2.5 while shaking overnight to elute the mAb and Et3i complex from the tip. Not only did this fail to remove all tip-bound species, but it also resulted in a much weaker binding of mAbs to the tip upon attempted reuse. This problem was solved through the development of a new regeneration strategy. In this procedure, tips were soaked immediately after use for 5 seconds in 20 mM glycine pH 1.5, and then 5 seconds in HBS. This process was then repeated 2-4 more times. With this strategy, tips showed nearly identical mAb loading to the tip relative to the last run they were used for and nearly zero complex binding to the tip. To perform the assays discussed in this work, new tips were purchased and the new regeneration method was employed. To eliminate the possibility of interference from previous experiments, the new biosensors were used for each trial prior to undergoing regeneration.

ITC Cooperativity Analysis of Anti-C2 Domain Inhibitors G99 and 3E6

To characterize the hypothesized cooperativity of inhibitors G99 and 3E6 in binding the C2 domain of FVIII, three different ITC experiments were carried out. These experiments included the titration of the 3E6 mAb into C2 WT, 3E6 mAb into C2 WT in complex with the G99 Fab, and the G99

mAb titrated into C2 WT. The proposed cooperativity occurs when G99 is bound to C2 and C2 subsequently binds another antibody, which is why no titration of the G99 mAb into C2 in complex with 3E6 was performed. The results for these three sets of titrations are outlined in Figures 17 and 18. Experimentally determined thermodynamic parameters for each experiment are outlined in Table 3.

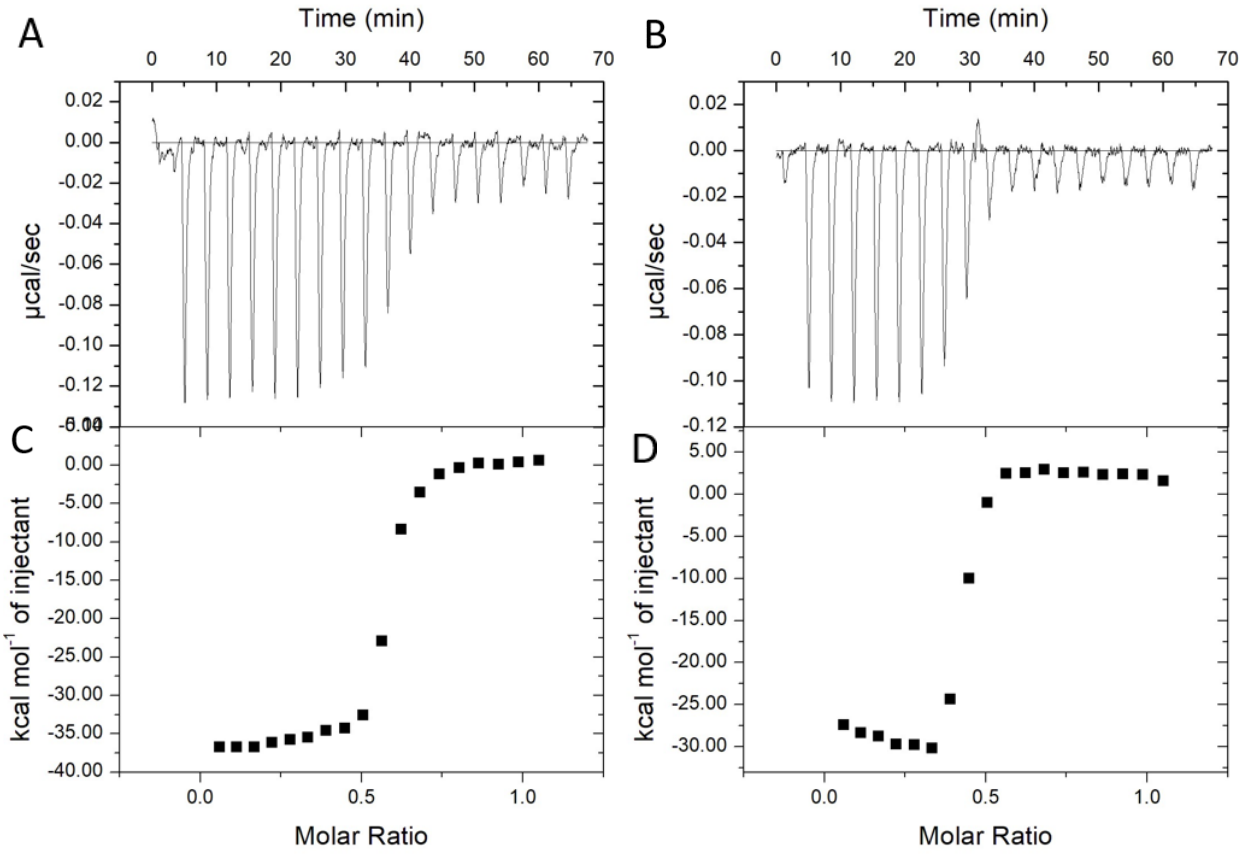

Figure 17. A) ITC thermogram of 3E6 mAb (6.25 µM) titrated into C2 WT (1.25 µM) at 35 °C. B) ITC thermogram of 3E6 mAb (6.25 µM) titrated into the C2-G99 Fab complex (1.25 µM) at 35 °C. C) Fitted binding curve for the 3E6 mAb into C2 WT. D) Fitted binding curve for the 3E6 mAb into C2-G99 Fab complex.

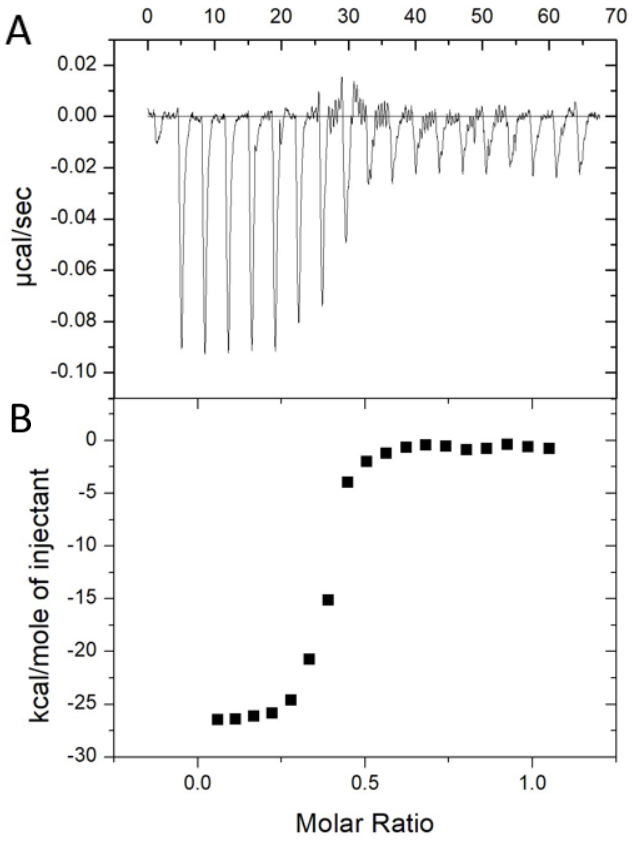

Figure 18. A) ITC thermogram of G99 mAb (6.25 µM) titrated into C2 WT (1.25 µM) at 35 °C. B) Fitted binding curve for the G99 mAb into C2 WT.

Table 3. Thermodynamic parameters for each ITC experiment as determined by ITC. N corresponds to the number of ligand molecules that bind to one macromolecule.

	ΔH (kcal/mol)	**TΔS (kcal/mol)**	**ΔG (kcal/mol)**	**K_D (nM)**	**N (sites)**
3E6 mAb + C2 WT	-36.23 ± 0.40	-2.71	-33.52	1.07 - 2.12	0.450
3E6 mAb + C2-G99 Fab	-29.88 ± 0.85	-1.98	-27.90	0.67 - 5.00	0.473
G99 mAb + C2 WT	-26.53 ± 0.30	-1.64	-24.89	1.96 - 4.38	0.369

When looking to analyze cooperativity between two ligands capable of simultaneously binding the same macromolecule, the cooperativity constant α must be mathematically determined using experimental thermodynamic or kinetic parameters. The simplest way to solve for α is to use Equation

1, which depends only on the rates of association (K_A) for 3E6 binding to C2, and 3E6 binding to the C2-G99 Fab complex ($K_{A/B}$).[42] However, due to the high affinity of 3E6 and C2, a reliable association rate was

$$K_{A/B} = \alpha K_A \quad (1)$$

unable to be determined for any of the binding experiments as the ability of ITC to accurately determine affinities ranges from low nanomolar to ~5 mM.[43] Since the steepness in the curve directly correlates to the rate of association, the slope of the binding curve only consisted of a few data points, introducing error significant enough to vary the apparent affinities and therefore heavily influence the value of α. A commonly encountered phenomenon when working with high-affinity systems is the production of aberrant signals around the inflection point of the binding curve. This can be seen in figure 18A during injections 8 and 9, where these injections had a significantly unstable baseline. This is likely the reason why valid K_Ds could not be determined for these interactions. This problem can sometimes be addressed through an increase in syringe stirring speed. Thus, a stirring speed increase from 351 to 500 rpm was attempted. But rather than fixing the issue, the high-stirring speed data proved to be far less reliable.

Experimental C-values for 3E6 and G99 were 195 and 77 respectively. C-values are a measurement of the reliability of affinity measurements made by ITC.[38] Typically, lower C-values (10-100) yield more reliable data. The C-value for G99 falls within this range and should give a reliable K_D, but did not most likely because its affinity is so tight. Unfortunately, too small of a signal was observed when decreasing the C-values of the 3E6 experiments, so reliable affinities could not be determined. Due to this observation, Equation 2 was used instead to calculate α as it depends largely on the free energy changes (ΔG), which proved to be far more consistent experimentally.[42] Additionally, this equation relies on the temperature (T) at which the experiment was performed, the concentration of the ligand pre-complexed to the macromolecule in the cell [B], and the association rate for the pre-complexed ligand binding to the macromolecule (K_B).[42] In this study, ΔG_A^{app} is the free-energy shift of 3E6 binding to C2-

G99, and ΔG_A is that of 3E6 binding to C2. K_B is the association rate for G99 to C2, and [B] is the concentration of G99 complexed to C2 in the cell. As previously stated, K_B is an unreliable variable, but in this equation seems to have little effect mathematically on the resulting value of α.

$$\Delta G_A^{app} = \Delta G_A - RT \ln \frac{1+\alpha K_B[B]}{1+K_B[B]} \quad (2)$$

Plugging experimental thermodynamic parameters into Equation 2, a value of 1.00 for α results, indicating that these two inhibitors likely have little influence on the binding of one another.[42] However, looking to the TΔS column in Table 3, it appears that the binding event associated with 3E6 binding to C2 becomes more entropically favorable if G99 is already present on each C2 molecule. The TΔS for 3E6 binding to C2 is -2.71 kcal/mol, while the TΔS for 3E6 binding to the C2-G99 complex is -1.98 kcal/mol. These values show a ~27% decrease in the disorder of the binding event, supporting the hypothesis that G99 works to rigidify the C2 domain upon its binding. This movement towards a more ordered system however, does not seem to significantly aid 3E6's binding of C2. In a cooperative system, it is common to see the K_D of the ligand decrease if there is a cooperating ligand pre-bound.[42] Unfortunately, this phenomenon cannot be fully addressed through this data as the range of K_D values for 3E6 binding to C2-G99 is too broad. The lower bound of this range, 0.67 nM, is tighter than the lower bound of 3E6 binding to C2 by itself. This would be a reasonable improvement in 3E6's affinity to C2, but the upper bound on this range is 5.00 nM, which would indicate that the affinity of 3E6 has lessened by nearly 50%. Additionally, the shift in free energy moves to a slightly less favorable state when 3E6 binds to C2-G99. Although the TΔS is more favorable, the ΔH seems to lessen and contribute more to the overall less favorable value of ΔG than the TΔS. As antibodies are designed by the body to bind to a given antigen in its native state with high specificity, the slight decrease in thermodynamic favorability could be a result of this. 3E6 is meant to bind to C2 in its usual flexible state, but when C2 rigidifies upon binding G99, C2 is no longer in its native state.

Aside from cooperativity analysis, it is worth noting that to our knowledge, this is the first instance of thermodynamic characterization of FVIII antibody-antigen interactions by ITC. Unlike BLI or SPR (Surface Plasmon Resonance), which require the immobilization of one protein as it prepares to bind its partner, ITC measures binding the kinetics and thermodynamics of free molecules interacting in solution. This advantage makes ITC a more accurate system when looking to measure events occurring in the human body, where molecules are free-floating rather than immobilized. BLI and SPR do however provide more reliable affinity measurements between high affinity ligands than ITC, making them the best choice for kinetic evaluations of these interactions. They also require far less protein than ITC, which is useful in the case of FVIII studies as FVIII in high abundance is difficult to procure.

Conclusions and Future Work

Hemophilia A is one of the most common inherited bleeding disorders worldwide, stemming from a deficiency or complete absence of coagulation factor VIII. As a result, hemophilia A patients suffer from uncontrolled bleeding episodes in their joints, muscles, and soft tissues. To treat this condition, patients must receive lifelong FVIII infusion therapy two to three times per week. During FVIII infusion therapy, patients are administered rFVIII or other products aiming to increase rates of clot formation. In the case of patients with severe hemophilia A, who constitute 60-70% of all hemophiliacs, FVIII inhibitors are often developed by the immune system upon reception of these injections. These inhibitors represent the greatest complication involved in FVIII infusion therapy, as they render the injected FVIII functionally ineffective. This phenomenon necessitates the development of next-generation therapeutics for use in FVIII infusion therapy that provide a lower likelihood of patient inhibitor development upon their administration while still filling FVIII's role in clot formation.

Inhibitors exist for each domain in FVIII, particularly the A2, C2, and A3-C1 domains. As each of these domains plays a different role in FVIII's function in the coagulation cascade, structural characterization of FVIII in complex with inhibitory antibodies provides valuable insight on mechanisms of inhibition. Through the understanding of inhibitory mechanisms displayed by anti-FVIII inhibitors, the possibility of designing a less immunogenic FVIII construct arises. With a less immunogenic FVIII to be used in FVIII infusion therapy, efficacy of the treatment could increase and alongside patient quality of life. The structural determination of the C1 domain in complex with the human inhibitory antibody NB2E9 via X-ray crystallography was attempted to further our knowledge on how antibodies produced by patients work to target the C1 domain of FVIII and inhibit its activity through the blockage of vWF and lipid binding. Although the produced crystals failed to diffract, a cryo-EM structure of human/porcine chimeric FVIII construct Et3i in complex with NB2E9 was solved by K. Childers in the Spiegel lab. This structure illustrated how the rare occurrence of glycosylation in inhibitors can play a crucial role in FVIII

inhibition. Although not interacting directly with FVIII, it is through this glycan that the D' region of vWF is blocked. When comparing this structure to that of Et3i:2A9, an antibody generated by hemophiliac mice when injected with human FVIII, striking similarities were revealed. This comparison highlights the commonalities between mammalian immune responses to rFVIII across species and may aid researchers in developing a less immunogenic construct of rFVIII to administer to hemophiliacs.

The FVIII A2 domain is the location in which thrombin activation of FVIII and binding of FIXa and FX occurs. Therefore, antibodies complementary to the A2 domain decrease or abolish FVIII activity through the disruption of one of these processes. To better understand how inhibitors compete with each other for binding of the FVIII A2 domain and what processes they may interfere with, a series of BLI competition assays was performed on antibodies 4A4, NB11B2, 4F4, 1D4, and 4C7. From this work, it was determined that antibody NB11B2 competes with group A antibody 4A4 for FVIII binding. As group A inhibitors interfere with the formation of the tenase complex, it is likely that NB11B2 disrupts this process in some way, despite its epitope not appearing to interfere with FIXa binding. NB11B2 interferes with the binding of group B antibody 4F4 to a lesser extent, suggesting that their epitopes do not completely overlap. Aside from NB11B2, 4A4 is capable of binding simultaneously with all listed inhibitors. 4F4 competition assays delivered conflicting results to those reported in the literature, as this inhibitor only seemed to block the binding of group E inhibitor 1D4. Group E inhibitors 1D4 and 4C7 were proven capable of binding simultaneously with all antibodies of study, outside of each other.

Given the recent success found by K. Childers in his solving of the cryo-EM structures of Et3i in complex with anti-C1 inhibitors NB33 and NB2E9 alongside NB11B2, the possibility of a solved cryo-EM structure of a FVIII ternary complex with two anti-A2 domain inhibitors seems within reach. While Cryo-EM studies on any of the complexes formed by simultaneously binding inhibitors could be attempted, a FVIII complex containing 4A4 and 1D4 may be the most insightful. Both antibodies have been studied extensively and potently inhibit FVIII activity, and their structures could provide valuable insight as to

why this is the case. 4A4 specifically most strongly inhibits FVIII with an inhibitor titer of 40,000 BU, while 1D4 has a titer of 11,000 BU.[17] Aside from 1D4, another candidate for this complex is the other group E antibody of study, 4C7. 4C7 is a non-inhibitory antibody with a titer of <1 BU and the solving of its structure with FVIII would provide indispensable information as to why certain antibodies do not inhibit FVIII as strongly as others when bound to the A2 domain. Looking to the studies performed using a mutant of LE2E9 as an antithrombotic to slow postoperative bleeding, weakly-inhibitory antibodies such as 4C7 may have similar utility in patients with excessive clotting disorders.

As the immune response to injected FVIII is polyclonal, it is possible that some of these inhibitors may cooperate with each other to inhibit FVIII function. Should cooperation be revealed, structural conformations conducive to inhibitor binding would be identified, laying the groundwork for the development of a less immunogenic FVIII. Based upon B-factor analysis of crystal structures of FVIII in complex with anti-C2 inhibitors 3E6 and G99, a possibility of cooperation between the two inhibitors was observed. This analysis suggested a rigidification of the C2 domain as G99 binds, potentially enabling 3E6 to bind more easily to the opposite side. This would have been the first instance of positive cooperativity observed between FVIII inhibitors and would provide valuable information regarding the polyclonal immune response to FVIII. To assess the nature of this interaction, ITC experiments were designed in which thermodynamic parameters ΔH, ΔG and TΔS were accurately determined for each antibody binding to FVIII on its own, and for 3E6 binding to the C2 domain in complex with G99. Using the ΔG and rate of association values from these experiments, the cooperativity constant α was calculated to be 1.00 for the binding of 3E6 to the C2-G99 complex. This value proves that the two inhibitors are cooperating in a neither positive or negative manner, and bind FVIII without influencing one another. In support of our hypothesis however, the TΔS for 3E6's binding of C2-G99 was less negative than that of C2 on its own, suggesting a less disordered C2 domain that could be attributed to rigidification. This perceived lack of cooperation between the two inhibitors alludes to a polyclonal

antibody response to FVIII that is specific to FVIII in its native state. These antibodies likely have paratopes that recognize native FVIII independently rather than in an altered conformation induced by the binding of a different antibody. As an alternative to this, it is still entirely possible that one antibody recognition of FVIII could potentially elicit a pernicious secondary immune recognition specific to an alternative conformation that is stabilized by the presence of an initial antibody complex, just not in the case of 3E6 and G99.

Works Cited

1. Gale, A. J. Continuing Education Course #2: Current Understanding of Hemostasis. Toxicologic Pathology 39, (2011).
2. Periayah, M. H. et al. Mechanism Action of Platelets and Crucial Blood Coagulation Pathways in Hemostasis. Int J Hematol. Oncol. Stem Cell Res. 2017; 11(4): 319–327.
3. Smith, S. A.; Travers, R. J.; Morrissey, J. H. How It All Starts: Initiation of the Clotting Cascade. Critical Reviews in Biochemistry and Molecular Biology 2015, 50 (4), 326–336.
4. Smith, S. A. The cell-based model of coagulation. Journal of Veterinary Emergency and Critical Care 19, (2009).
5. Palta, S.; Saroa, R.; Palta, A. Overview of the Coagulation System. Indian Journal of Anaesthesia 2014, 58 (5), 515.
6. Novakovic, V. A.; Cullinan, D. B.; Wakabayashi, H.; Fay, P. J.; Baleja, J. D.; Gilbert, G. E. Membrane-Binding Properties of the Factor VIII C2 Domain. The Biochemical journal 2011, 435 (1), 187–196.
7. Orlova, N. A.; Kovnir, S. V.; Vorobiev, I. I.; Gabibov, A. G.; Vorobiev, A. I. Blood Clotting Factor VIII: From Evolution to Therapy. Acta Naturae 2013, 5 (2), 19–39.
8. Youssoufian, H.; Antonarakis, S. E.; Aronis, S.; Tsiftis, G.; Phillips, D. G.; Kazazian, H. H. Characterization of Five Partial Deletions of the Factor VIII Gene. Proceedings of the National Academy of Sciences of the United States of America 1987, 84 (11), 3772–3776.
9. PIPE, S. W. Functional Roles of the Factor VIII B Domain. Haemophilia 2009, 15 (6), 1187–1196.
10. Shen, B. W.; Spiegel, P. C.; Chang, C.-H.; Huh, J.-W.; Lee, J.-S.; Kim, J.; Kim, Y.-H.; Stoddard, B. L. The Tertiary Structure and Domain Organization of Coagulation Factor VIII. Blood 2008, 111 (3), 1240–1247.

11. Jardim, L. L.; Chaves, D. G.; Rezende, S. M. Development of Inhibitors in Hemophilia A: An Illustrated Review. Research and Practice in Thrombosis and Haemostasis 2020, 4 (5), 752–760.
12. Yousphi, A. S.; Bakhtiar, A.; Cheema, M. A.; Nasim, S.; Ullah, W. Acquired Hemophilia A: A Rare but Potentially Fatal Bleeding Disorder. Cureus 2019, 11 (8).
13. Butterfield, J. S. S.; Hege, K. M.; Herzog, R. W.; Kaczmarek, R. A Molecular Revolution in the Treatment of Hemophilia. Molecular Therapy 2019.
14. Schep, S. J.; Schutgens, R. E. G.; Fischer, K.; Boes, M. L. Review of Immune Tolerance Induction in Hemophilia A. Blood Reviews 2018, 32 (4), 326–338.
15. Dargaud, Y.; Escuriola-Ettingshausen, C. Recombinant Porcine Factor VIII: Lessons from the Past and Place in the Management of Hemophilia a with Inhibitors in 2021. Research and Practice in Thrombosis and Haemostasis 2021, 5 (8).
16. Franchini, M. Plasma-Derived versus Recombinant Factor VIII Concentrates for the Treatment of Haemophilia A: Recombinant Is Better. Blood Transfusion 2010, 8 (4), 292–296.
17. Doering, C. B.; Healey, J. F.; Parker, E. T.; Barrow, R. T.; Lollar, P. Identification of Porcine Coagulation Factor VIII Domains Responsible for High Level Expression via Enhanced Secretion. Journal of Biological Chemistry 2004, 279 (8), 6546–6552.
18. Konkle, B. A.; Stasyshyn, O.; Chowdary, P.; Bevan, D. H.; Mant, T.; Shima, M.; Engl, W.; Dyck-Jones, J.; Fuerlinger, M.; Patrone, L.; Ewenstein, B.; Abbuehl, B. Pegylated, Full-Length, Recombinant Factor VIII for Prophylactic and On-Demand Treatment of Severe Hemophilia A. Blood 2015, 126 (9), 1078–1085.
19. Chowdary, P.; Fosbury, E.; Riddell, A.; Mathias, M. Therapeutic and Routine Prophylactic Properties of rFactor VIII Fc (Efraloctocog Alfa, Eloctate®) in Hemophilia A. Journal of Blood Medicine 2016, (7), 187–198.

20. Leissinger, C. A.; Singleton, T.; Kruse-Jarres, R. How I Use Bypassing Therapy for Prophylaxis in Patients with Hemophilia A and Inhibitors. Blood 2015, 126 (2), 153–159.
21. Antunes, S. V.; Tangada, S.; Stasyshyn, O.; Mamonov, V.; Phillips, J.; Guzman-Becerra, N.; Grigorian, A.; Ewenstein, B.; Wong, W.-Y. Randomized Comparison of Prophylaxis and On-Demand Regimens with FEIBA NF in the Treatment of Haemophilia A and B with Inhibitors. Haemophilia 2014, 20 (1), 65–72.
22. Konkle, B. A.; Ebbesen, L. S.; Erhardtsen, E.; Bianco, R. P.; Lissitchkov, T.; Rusen, L.; Serban, M. A. Randomized, Prospective Clinical Trial of Recombinant Factor VIIa for Secondary Prophylaxis in Hemophilia Patients with Inhibitors: Factor VIIa Prophylaxis in Hemophilia. Journal of Thrombosis and Haemostasis 2007, 5 (9), 1904–1913.
23. Food and Drug Administration. FDA Approves First Gene Therapy for Adults with Severe Hemophilia A. FDA 2023.
24. Vidarsson, G.; Dekkers, G.; Rispens, T. IgG Subclasses and Allotypes: From Structure to Effector Functions. Frontiers in Immunology 2014, 5 (1).
25. Witmer, C.; Young, G. Factor VIII Inhibitors in Hemophilia A: Rationale and Latest Evidence. Therapeutic Advances in Hematology 2012, 4 (1), 59–72.
26. Markovitz, R. C.; Healey, J. F.; Parker, E. T.; Meeks, S. L.; Lollar, P. The Diversity of the Immune Response to the A2 Domain of Human Factor VIII. Blood 2013, 121 (14), 2785–2795.
27. Coxon, C. H.; Yu, X.; Beavis, J.; L. Diaz-Saez; Riches-Duit, A.; Ball, C.; Diamond, S. L.; Raut, S. Characterisation and Application of Recombinant FVIII-Neutralising Antibodies from Haemophilia a Inhibitor Patients. 2021, 193 (5), 976–987.
28. Batsuli, G.; Deng, W.; Healey, J. F.; Parker, E. T.; Baldwin, W. H.; Cox, C.; Nguyen, B.; Kahle, J.; Königs, C.; Li, R.; Lollar, P.; Meeks, S. L. High-Affinity, Noninhibitory Pathogenic C1 Domain

Antibodies Are Present in Patients with Hemophilia a and Inhibitors. Blood 2016, 128 (16), 2055–2067.

29. Gilbert, G. E. Factor VIII–Antibody Structure and Membrane Binding. Blood 2021, 137 (21), 2866–2868.
30. Jacquemin, M.; Benhida, A.; Peerlinck, K.; DesqueperB.; Vander Elst, L.; Lavend'homme, R.; d'Oiron, R.; Schwaab, R.; Bakkus, M.; Thielemans, K.; Gilles, J.-G.; Vermylen, J.; Saint-Remy, J.-M. A Human Antibody Directed to the Factor VIII C1 Domain Inhibits Factor VIII Cofactor Activity and Binding to von Willebrand Factor. Blood 2000, 95 (1), 156–163.
31. Jacquemin, M.; Radcliffe, C. M.; Renaud Lavend'homme; Wormald, M.; Luc VanderElst; Goedele Wallays; Dewaele, J.; Collen, D.; Jozef Vermylen; Dwek, R. A.; Jean-Marie Saint-Remy; Rudd, P. M.; Mieke Dewerchin. Variable Region Heavy Chain Glycosylation Determines the Anticoagulant Activity of a Factor VIII Antibody. 2006, 4 (5), 1047–1055.
32. Gilbert, G.E.; Bhimavarapu, A.; Price, P.; Jacquemin, M. Antibody to C1 Domain of Factor VIII Alters Interaction of Factor Xase Complex with Factor X. Blood 2004, 104 (11), 1738.
33. Smyth, M. S.; Martin, J. H. J. X Ray Crystallography. Molecular Pathology 2000, 53 (1), 8–14.
34. Raimondi, V.; Grinzato, A. A Basic Introduction to Single Particles Cryo-Electron Microscopy. AIMS Biophysics 2021, 9 (1), 5–20.
35. Boldon, L.; Laliberte, F.; Liu, L. Review of the Fundamental Theories behind Small Angle X-Ray Scattering, Molecular Dynamics Simulations, and Relevant Integrated Application. Nano Reviews 2015, 6 (1), 25661.
36. Ronayne, E. K.; Peters, S. C.; Gish, J. S.; Wilson, C.; Spencer, H. T.; Doering, C. B.; Lollar, P.; Spiegel, P. C.; Childers, K. C. Structure of Blood Coagulation Factor VIII in Complex with an Anti-C2 Domain Non-Classical, Pathogenic Antibody Inhibitor. Frontiers in Immunology 2021, 12, 697602.

37. Walter, J. D.; Werther, R. A.; Brison, C. M.; Cragerud, R. K.; Healey, J. F.; Meeks, S. L.; Lollar, P.; Spiegel, P. C. Structure of the Factor VIII C2 Domain in a Ternary Complex with 2 Inhibitor Antibodies Reveals Classical and Nonclassical Epitopes. Blood 2013, 122 (26), 4270–4278.
38. Archer, W. R.; Schulz, M. D. Isothermal Titration Calorimetry: Practical Approaches and Current Applications in Soft Matter. Soft Matter 2020, 16 (38), 8760–8774.
39. Kahle, J.; Orlowski, A.; Stichel, D.; Healey, J. H.; Parker, E. T.; Jacquemin, M.; Krause, M.; Tiede, A.; Schwabe, D.; Lollar, P.; Christoph Königs. Frequency and Epitope Specificity of Anti–Factor VIII C1 Domain Antibodies in Acquired and Congenital Hemophilia A. 2017, 130 (6), 808–816.
40. Huang, Z.; Gengenbach, T.; Tian, J.; Shen, W.; Garnier, G. Effect of Bovine Serum Albumin Treatment on the Aging and Activity of Antibodies in Paper Diagnostics. Frontiers in Chemistry 2018, 6.
41. Jacquemin, M. et al. U.S. Patent No. US7858089B2 (2010).
42. Velazquez-Campoy, A.; Goñi, G.; Peregrina, J. R.; Medina, M. Exact Analysis of Heterotropic Interactions in Proteins: Characterization of Cooperative Ligand Binding by Isothermal Titration Calorimetry. Biophysical Journal 2006, 91 (5), 1887–1904.
43. Hevener, K. E.; Pesavento, R.; Ren, J.; Lee, H.; Ratia, K.; Johnson, M. E. Hit-To-Lead: Hit Validation and Assessment. Methods in Enzymology 2018, 265–309.